



1 **Trends analysis of PM source contributions and chemical tracers in NE Spain during 2004 - 2014: A multi-**
2 **exponential approach.**

3

4 Marco Pandolfi^{1,*}, Andrés Alastuey¹, Noemi Pérez¹, Cristina Reche¹, Iria Castro¹, Victor Shatalov² and Xavier Querol¹

5 ¹ Institute of Environmental Assessment and Water Research, c/ Jordi-Girona 18-26, 08034 Barcelona, Spain

6 ² Meteorological Synthesizing Centre – East, 2nd Roshchinsky proezd, 8/5, 115419 Moscow, Russia

7 *Corresponding author: marco.pandolfi@idaea.csic.es

8

9

10

11 **Abstract**

12 In this work for the first time data from two twin stations (Barcelona, urban background, and Montseny,
13 regional background), located in NE of Spain, were used to study the trends of the concentrations of different
14 chemical species in PM₁₀ and PM_{2.5} along with the trends of the PM₁₀ source contributions from Positive Matrix
15 Factorization (PMF) model. Eleven years of chemical data (2004–2014) were used for this study. Trends of both
16 specie concentrations and source contributions were studied using the Mann-Kendall test for linear trends and
17 a new approach based on multi-exponential fit of the data. Despite the fact that different PM fractions (PM₁,
18 PM_{2.5}, PM₁₀) showed linear decreasing trends at both stations, the contributions of specific sources of pollutants
19 and the related chemical tracers showed exponential (single or double) decreasing trends. The different types
20 of trends observed reflected the different effectiveness and/or time of implementation of the measures taken
21 to reduce the concentrations of atmospheric pollutants (i.e. those implemented in the Industrial Emission
22 Directives and in the Large Combustion Plants Directive). Moreover, the trends of the contributions from
23 specific sources such as those related with industrial activities and with primary energy consumption mirrored
24 the effect of the financial crisis in Spain from 2008. The sources that showed statistically significant downward
25 trends at both Barcelona (BCN) and Montseny (MSY) during 2004–2014 were *Ammonium sulfate*, *Ammonium*
26 *nitrate*, and *V-Ni bearing* source. The contributions from these sources decreased exponentially during the
27 considered period indicating that the observed decrease was not gradual and consistent over time. Moreover,
28 statistically significant decreasing trends were observed for the contributions to PM from the *Industrial/Traffic*
29 source at MSY (mixed metallurgy and road traffic) and from the *Industrial* (metallurgy mainly) source at BCN.
30 These sources were clearly linked with anthropogenic activities and the observed decreasing trends confirmed
31 the effectiveness of pollution control measures implemented at EU or regional/local levels. The general trends
32 observed for the calculated PMF source contributions well reflected the trends observed for the chemical
33 tracers of these pollutant sources.

34



35 1. Introduction

36 Meeting the air quality (AQ) standards is one of the major environmental objectives to protect people from
37 breathing air with high levels of pollution. Many studies have been published in these last years showing clearly
38 that the concentrations of particulate matter (PM), and other air pollutants such as sulphur dioxide (SO₂) and
39 carbon monoxide (CO), have markedly decreased during the last 15 years in many European Countries (EEA,
40 2013; Barmpadimos et al., 2012; Cusack et al., 2012; Querol et al., 2014; Guerreiro et al., 2014 among others).
41 Cusack et al. (2012) reported the reduction in PM_{2.5} concentrations observed at regional background (RB)
42 stations in Spain and across Europe, and, in most cases, the observed reduction was gradual and consistent over
43 time, implying the success of cleaner anthropogenic activities. Barmpadimos et al. (2012) have also shown that
44 PM₁₀ concentrations decreased at a number of urban background (UB) and rural background stations in five
45 European countries. Henschel et al. (2013) reported the dramatic decrease in SO₂ levels across six European
46 cities, reflecting the reduction in sulphur content in fuels, as part of EU legislation, coupled with the shift
47 towards the use of cleaner fuels. EEA (2013) also reported general decreases in NO₂ concentrations even if
48 lower compared to PM. However, Henschel et al. (2015) showed that the NO_x concentrations at traffic sites in
49 many EU cities remained unchanged underlining the need of further regulative measures to meet the air quality
50 standards for this pollutant. In fact an important proportion of the European population lives in areas exceeding
51 the AQ standards for the annual limit value of NO₂, the daily limit value of PM₁₀ and the health protection
52 objective of O₃ (EEA, 2013; 2015). PM₁₀ and NO₂ are still exceeded mostly in urban areas, and especially at
53 traffic sites (Harrison et al., 2008; Williams and Carslaw, 2011; EEA, 2013; among others). In Spain for example it
54 has been reported that more than 90% of the NO₂ exceedances are attributed to road traffic emissions (Querol
55 et al., 2012). Guerreiro et al. (2014) furthermore evidenced notable reduction of ambient air concentration of
56 SO₂, CO and Pb using data available in Airbase (EEA, 2013) and covering 38 European countries. Querol et al.
57 (2014) reported trends for 73 measurement sites across Spain including RB, UB, traffic stations (TS) and
58 Industrial sites (IND). They observed marked downward concentration trends for PM₁₀, PM_{2.5}, CO and SO₂ at
59 most of the RB, UB, TR and IND sites considered. Similarly, Salvador et al. (2012) detected a statistically
60 significant downward trends in the concentrations of SO₂, NO_x, CO and PM_{2.5} at most of the urban and urban-
61 background monitoring sites in the Madrid metropolitan area during 1999-2008. Cusack et al. (2012) and Querol
62 et al. (2014) have also shown the highly statistically significant decreasing trends observed at regional level in
63 NE Spain for many trace elements since 2002 (Pb, Cu, Zn, Mn, Cd, As, Sn, V, Ni, Cr).

64 The observed reduction of air pollutants across Europe is the results of efficient emission abatement strategies
65 as for example those implemented in the Industrial Emission Directives (IPPC Integrated Pollution Prevention
66 and Control and subsequent Industrial Emission Directives 1996/61/EC and 2008/1/EC), the Large Combustion
67 Plants Directive (LCPD; 2001/80/EC), the EURO standards on road traffic emission (1998/69/EC, 2002/80/EC,
68 2007/715/EC), the IMO (International Maritime Organization) directive on sulphur content in fuel, and SO_x and
69 NO_x emissions from ships (IMO, 2011; Directive 2005/33/EC). Additionally, the financial crisis, causing mainly a



70 reduction of the primary energy consumption from 2008-2009, contributed to the decrease of the ambient
71 concentration of pollutants observed in Spain (Querol et al., 2014).

72 Moreover, national and regional measures for AQ have been taken in many European Countries. In Spain a
73 national AQ plan was approved in 2011 and updated in 2013 by the Council of Ministers of the Government of
74 Spain. Furthermore, 45 regional and 3 local (city scale) AQ plans have been implemented since 2004 in Spain.
75 These AQ Plans mostly focused on improving AQ at major city centers or specific industrial areas.

76 For the aforementioned reasons, it is especially attractive the feasibility of studying the trends of the
77 contributions to PM mass from specific pollutant sources along with the trends of the chemical tracers of these
78 sources.

79 A repository of previous works studying the trends of atmospheric pollutants is reported in the Wikipedia of *The*
80 *Task Force on Measurements and Modelling* (TFMM; [https://wiki.met.no/emep/emep-](https://wiki.met.no/emep/emep-experts/tfmmtrendpublis)
81 [experts/tfmmtrendpublis](https://wiki.met.no/emep/emep-experts/tfmmtrendpublis)). The TFMM together with the *Task Force on Emission Inventories and Projections*
82 (TFEIP), the *Task Force on Integrated Assessment Modelling* (TFIAM), and *Task Force on Hemispheric Transport*
83 *of Air Pollution* (TFHTAP) provide a fora for discussion and scientific exchange in support of the EMEP (*European*
84 *Monitoring and Evaluation Programme*; <http://www.emep.int/>) work plan which is a scientifically based and
85 policy driven programme under the *Convention on Long-range Transboundary Air Pollution* (CLRTAP;
86 http://www.unece.org/env/lrtap/lrtap_h1.html) promoting the international co-operation to solve
87 transboundary air pollution problems. The TFMM was established in 2000 to evaluate measurements and
88 modeling and to further develop working methods and tools. In this contest, five EMEP Centers are undertaking
89 efforts in support of the EMEP work plan, namely the *Centre on Emission Inventories and Projections* (CEIP;
90 <http://www.ceip.at/>), the *Chemical Coordinating Centre* (CCC; <http://www.nilu.no/projects/ccc/>), the
91 *Meteorological Synthesizing Centre – West* (MSC-W; http://emep.int/mscw/index_mscw.html), the
92 *Meteorological Synthesizing Centre – East* (MSC-E; <http://www.msceast.org/>), and the *Centre for Integrated*
93 *Assessment Modelling* (CIAM; <http://www.iiasa.ac.at/~rains/ciam.html>). In 2014, the TFMM initiated a
94 dedicated exercise to assess the efficiency of air pollution mitigation strategies over the past 20 years to assess
95 the benefit of the CLRTAP main policy instrument. Within this exercise a software was made available by
96 EMEP/MSC-E Center aiming at studying non-linear trends and specifically using multi-exponential fits
97 (<https://wiki.met.no/emep/emep-experts/tfmmtrendmethods>).

98 For what we are concerned in the majority of studies dealing with trend analysis, linear fits were applied for
99 example by using Mann-Kendall or Theil-Sen methods (Theil, 1950; Sen, 1968), the latter being available for
100 example in the Openair software (Carslaw, 2012; Carslaw and Ropkins, 2012). However, linear fit of data does
101 not always properly represent the observed trends. As we will show, different abatement strategies and periods
102 of implementation may change from one pollutant to another thus leading to different trends for different
103 pollutants, even over the same period. Thus, non-linear fit of the data may be at times strongly recommended.



104 In this work we studied the trends of source contributions to PM_{10} and specific chemical species in both PM_{10}
105 and $PM_{2.5}$ using both the consensus methodology (Mann-Kendall) and the multi-exponential approach. PM
106 chemical speciated data collected from 2004 to 2014 at regional (Montseny; NE Spain) and urban (Barcelona,
107 NE Spain) sites were used with this aim. The selected period allowed for trend analysis at these twin stations
108 over a common period. The Positive Matrix Factorization (PMF) model was used to apportion ambient PM_{10}
109 concentrations into pollutant sources. The PMF model, as other Receptor Models (RM), is widely used being a
110 powerful tool to help policy makers to design more targeted approaches to protecting public health. Thus, the
111 novelty of this study lies mainly in a) the opportunity to study the trends of source contributions from PMF
112 model at two twin stations representative of the urban and regional environments in the Western
113 Mediterranean, and, b) in the use of a novel non-linear approach for trend studies.

114

115 2. Measurement sites and Methodology

116 2.1 Measurement sites

117 The Montseny measurement station (MSY, 41°46'45.63" N, 02°21'28.92" E, 720 m a.s.l.) is a regional
118 background site in NE of Spain (Figure 1). The MSY station is located within a regional natural park about 50 km
119 to the NNE of the city of Barcelona (BCN) and 25 km from the Mediterranean coast. This site is representative of
120 the typical regional background conditions of the Western Mediterranean Basin (WMB) characterized by severe
121 pollution episodes affecting not only the coastal sites closest to the emission sources, but also the more
122 elevated rural and remote areas land inwards due to thermally driven winds (i.e. Pérez et al., 2008; Pey et al.,
123 2010; Pandolfi et al., 2011; 2014). This station is part of ACTRIS (www.actris.net) and GAW (www.wmo.int/gaw)
124 networks, EMEP (<http://www.emep.int/>) and the measuring network of the Government of Catalonia.

125 The Barcelona measurement station (BCN, 41°23'24.01" N, 02°06'58.06" E, 68 m a.s.l.) is an urban background
126 measurement site influenced by vehicular emissions from one of the main avenues of the city (Diagonal
127 Avenue) located at a distance of around 300 m (cf. Fig. 1). The BCN measurement site is part of the Air Quality
128 measuring network of the Government of Catalonia. The Metropolitan Area of Barcelona (BMA), with nearly 4.5
129 million inhabitants, covers an 8 km wide strip between the Mediterranean Sea and the coastal mountain range.
130 Several industrial zones, power plants, and highways are located in the area, making this region to one of the
131 most polluted in the WMB (i.e. Querol et al., 2008; Amato et al., 2009; Pandolfi et al., 2012; 2013; 2014). At BCN
132 the location of the measuring station changed in 2009 when it was moved by around 500 m (cf. Fig. 1). The
133 effect of this change on PM measurements performed at BCN will discuss later.

134

135

136



137 **2.2 Real-time and gravimetric PM measurements**

138 Real-time PM concentrations were continuously measured at 1h resolution by optical particle counters (OPC)
139 using GRIMM spectrometers (GRIMM 180 at MSY, and GRIMM 1107, 1129 and 180 at BCN). Hourly PM
140 concentrations were corrected by comparison with 24h gravimetric mass measurements of PM_x (Alastuey et al.,
141 2011).

142 For gravimetric measurements 24h PM_x samples were collected at both stations every 3-4 days on 150 mm
143 quartz micro-fiber filters (Pallflex QAT and Whatman) with a high-volume (Hi-Vol) samplers (DIGITEL DH80
144 and/or MCV CAV-A/MSb at 30 m³h⁻¹). The mass of PM₁₀ and PM_{2.5} samples collected on filters was determined
145 using the EN 12341 and the EN14907 gravimetric procedures, respectively.

146

147 **2.2.1 PM chemical speciated data**

148 Once the gravimetric mass was determined from filters, the samples were analyzed with different techniques
149 including acidic digestion (½ of each filter; HNO₃:HF:HClO₄), water extraction of soluble anions (¼ of each filter),
150 and thermal-optical analysis (1.5 cm² sections). Inductively Coupled Atomic Emission Spectrometry, ICP-AES,
151 (IRIS Advantage TJA Solutions, THERMO) was used for the determination of the major elements (Al, Ca, Fe, K,
152 Na, Mg, S, Ti, P), and Inductively Coupled Plasma Mass Spectrometry, ICP-MS, (X Series II, THERMO) for the
153 trace elements (Li, Ti, V, Cr, Mn, Co, Ni, Cu, Zn, As, Se, Rb, Sr, Cd, Sn, Sb, Ba, rare earths, Pb, Bi, Th, U). Ionic
154 Chromatography was used for the concentrations of NO₃⁻, SO₄²⁻ and Cl⁻, whereas NH₄⁺ was determined using a
155 specific electrode MODEL 710 A+, THERMO Orion. The levels of OC and EC were determined by a thermal-
156 optical carbon analyzer (SUNSET), using protocol EUSAAR_2. Other analytical details may be found in Querol et
157 al. (2009).

158 Following the above procedures, PM₁₀ and PM_{2.5} chemical speciated data were obtained at MSY for the period
159 2004-2014 resulting in 1093 and 794 samples, respectively. At BCN PM₁₀ and PM_{2.5} data were obtained during
160 2004-2014 resulting in 1037 and 1063 samples, respectively.

161

162 **2.3 Positive Matrix Factorization (PMF) model.**

163 The PMF model (PMFv5.0, EPA) was used on the collected daily speciated data for source identification and
164 apportionment in PM₁₀ at both sites. Detailed information about the PMF model can be found in literature
165 (Paatero and Tapper 1994; Paatero 1997; Paatero and Hopke 2003; Paatero et al. 2005). The PMF model is a
166 factor analytical tool reducing the dimension of the input matrix in a limited number of factors (or sources) and
167 it is based on the weighted least-squares method. Thus, most important in PMF applications is the estimation of
168 uncertainties of the chemical species included in the input matrix. In the present study, individual uncertainties



169 and detection limits were calculated as in Escrig et al. (2009) and Amato et al. (2009). Thus, both the analytical
170 uncertainties and the standard deviations of species concentrations in the blank filters were considered in the
171 uncertainties calculations. The signal-to-noise ratio (S/N) was estimated starting from the calculated
172 uncertainties and used as a criteria ($S/N > 2$) for selecting the species used within the PMF model. In order to
173 avoid any bias in the PMF results, the data matrix was uncensored (End user's guide to multilinear engine
174 applications from Pentti Paatero). The PMF was run in robust mode (Paatero 1997), and rotational ambiguity
175 was handled by means of the F_{PEAK} parameter (Paatero et al. 2005). The optimal number of sources was selected
176 by inspecting the variation of the objective function Q (defined as the ratio between residuals and errors in each
177 data value) with varying number of sources (i.e. Paatero et al., 2002) and by studying the physical
178 meaningfulness of the calculated factors.

179 **2.4 Mann-Kendall (MK) fit**

180 The purpose of the Mann-Kendall (MK) test (Mann 1945, Kendall 1975, Gilbert 1987) is to statistically assess if
181 there is a monotonic upward or downward trend of the variable of interest over time. A monotonic upward
182 (downward) trend means that the variable consistently increases (decreases) through time.

183

184 **2.5 Multi-exponential (ME) fit**

185 A Program aiming at studying trends of time series of air pollution in the multi-exponential form was developed
186 within the TFMM by MSC-E group (Shatalov et al., 2015). Annual, monthly and daily resolution data can be
187 analyzed with the help of this program. Since in this paper we will apply the program to annual averages of
188 specie concentrations and source contributions, we restrict the description of the multi-exponential
189 approximations for this case. In particular, seasonal variations are not included into consideration. The basic
190 equations solved by the program for this particular case (annual averages) are reported below:

191

$$192 \quad C_t = a_1 \cdot \exp\left(-\frac{t}{\tau_1}\right) + a_2 \cdot \exp\left(-\frac{t}{\tau_2}\right) + \dots + a_n \cdot \exp\left(-\frac{t}{\tau_n}\right) + \omega_t \quad (1)$$

193

194 Where, C_t are the values of the considered time series, with $t = 1, \dots, N$, N being the length of the series (years),
195 τ_n are the characteristic times of the considered exponential, and a_n are constants. In the case of single
196 exponential decay ($n=1$) the characteristic time τ is the time at which the pollutant concentration is reduced to
197 $1/e$ ($= 0.3678$) times its initial value. Both τ_n and a_n are calculated by the program by means of the least square
198 method minimizing the residue ω . The number of exponential terms that should be included into the
199 approximation can be evaluated using F -statistics (i.e. Smith, 2002). For example, the F -statistics for the
200 evaluation of the statistical significance of the second term in equation (1) for $n = 2$ can be calculated as:



201

$$202 \quad F = \frac{(SS_1 - SS_2)}{2 \cdot s} \quad (2)$$

203

204 where SS_1 and SS_2 are sums of squares of residual component for approximations with one and two exponential
 205 terms, respectively, and s is the estimate of standard deviation of residual component. This statistics follows
 206 approximately the Fisher distribution with 2 and $N - 2$ degrees of freedom. Second exponential is considered to
 207 be significant if F exceeds the corresponding threshold value at the chosen significance level.

208 The following parameters can be calculated from equation (1):

$$209 \quad - \text{ Total Reduction (TR):} \quad TR = \frac{(C_{beg} - C_{end})}{C_{beg}} = 1 - \frac{C_{end}}{C_{beg}} \quad (3)$$

$$210 \quad - \text{ Annual reduction for year } i: \quad R_i = \frac{\Delta C_i}{C_i} = 1 - \frac{C_{i+1}}{C_i} \quad (4)$$

$$211 \quad - \text{ Average annual reduction:} \quad R_{av} = 1 - \left(\frac{C_{end}}{C_{beg}} \right)^{\frac{1}{N-1}} \quad (5)$$

212 The formula for calculation of average annual reduction takes into account that the ratio C_{i+1} / C_i is a
 213 multiplicative quantity, so that geometrical mean of ratios should be used.

214 The MSC-E also proposed a statistic which can be used to check if the trends are linear or not (Non-Linearity:
 215 NL). More detailed description of the multi-exponential approach is available in the TFMM wiki and in the MSC-
 216 E Technical report 2015 (Shatalov et al., 2015).

217

218 3. Results

219 Results will be presented and discussed in the following order: First (*Paragraph 3.1*), we will compare the trends
 220 at both stations of PM_x concentrations from optical counters (OPC; annual data coverage around 90%) and from
 221 24h gravimetric samples (filters; annual data coverage around 20-30%). This comparison will demonstrate the
 222 feasibility of studying trends of pollutant concentrations from filters analyses despite the relatively low annual
 223 data coverage. Second (*Paragraph 3.2*), we will compare the magnitude of the trend of $PM_{2.5}$ concentrations at
 224 MSY during 2004-2014 (period selected for this study) with the magnitude of trends calculated at the same
 225 station over different periods, namely 2002-2010 (the period used in Cusack et al., 2012) and 2002-2014
 226 (representing the largest period of gravimetric $PM_{2.5}$ measurements available so far at MSY station). This
 227 comparison was performed in order to study the effects of meteorology on the magnitude of the trends over
 228 relatively short periods. The gravimetric concentrations of $PM_{2.5}$ were used with this aim. Third, we will present
 229 and discuss the trends at both stations of chemical species in both PM_{10} and $PM_{2.5}$ from 24h filter analyses
 230 (*Paragraph 3.3*). Fourth, we will discuss the sources of pollutants identified by PMF model in PM_{10} at both sites



231 (*Paragraph 4.0*). Finally, we will present and discuss the trends of PM₁₀ source contributions at BCN and MSY
232 (*Paragraph 4.1*). In *Paragraph 4.1* we will provide possible explanations for the observed trends.

233

234 **3.1 Trends of PM: Comparison between gravimetric and real-time optical measurements**

235 In this section we evaluate the feasibility of studying the trends of PM concentrations from gravimetric samples
236 by comparing the trends of 24h PM concentrations from filters to those obtained using daily averaged real-time
237 data from optical counters (OPC). In fact, the annual coverage of gravimetric measurements was around 30% at
238 both sites, whereas the OPC measurements had an annual coverage of around 90%. Note that the
239 recommended annual data coverage for trend studies is typically 75%.

240 Table 1 reports the trends (during 2004-2014) of annual mean concentrations of different PM size fractions
241 (from both OPC and gravimetric measurements) at both BCN and MSY calculated using both the Mann-Kendall
242 (MK) and multi-exponential (ME) fits. Gravimetric PM₁ concentrations were not available for the whole period
243 and only OPC data were reported in Table 1. Similarly, calculated PM_x concentrations (PM₁₋₁₀ and PM_{2.5-10}) and
244 PM ratios (PM₁/PM₁₀ and PM_{2.5}/PM₁₀) were reported only for OPC data. Following the MK test, statistically
245 significant decreasing trends were observed for all PM size fractions at BCN (ranging from -2.18 %/yr with
246 p<0.05 for PM_{2.5-10} to -3.89 %/yr with p<0.001 for PM_{2.5}), whereas at Montseny only the PM_{2.5} fraction showed a
247 statistical significant decreasing trend (-1.87 %/yr, p<0.1 from gravimetric measurements). The higher
248 statistical significance of the PM_x trends observed at BCN compared to MSY was likely due to the change of
249 the measuring station in 2009 in BCN (cf. Fig. 1). Based on the comparison between simultaneous PM_x chemical
250 speciated data collected at both BCN measurement sites during 1 month (not shown) we concluded that after
251 2009 the BCN measuring site was less affected by mineral matter and, to a lesser extent, by road traffic
252 emissions both being important sources of PM in Barcelona. In Figure 1 we highlighted the proximity of the BCN
253 measuring station before 2009 to an unpaved parking and different construction works. The effect of the
254 change of the station in BCN in 2009 on PM₁₀ gravimetric measurements was reported in Supporting
255 Information (Figure SI-1). Thus, we will discuss here the magnitude of the trends of PM_x concentrations at MSY
256 only. However, despite the change of station, the comparison between BCN and MSY for specific chemical
257 species and pollutant sources not linked with these two pollutant sources (mineral matter and road traffic
258 emissions) was possible.

259 Table 1 shows that the trends of different PM_x size fractions at MSY were linear (L) during the period 2004-
260 2014. In fact the non-linearity parameter (NL), which is an estimation of how much the trend differs from the
261 linear one, was always lower than 10% which was used as threshold for non-linearity (Shatalov et al., 2015). The
262 characteristic times (τ) from ME fit of PM_x reported in Table 1 were not directly comparable between BCN and
263 MSY again because of the change of the station occurred in BCN in 2009. As a consequence the characteristic
264 times (τ) for PM₁, PM_{2.5} and PM₁₀ at BCN were much lower than at MSY indicating a steeper decrease of PM_x



265 concentrations at BCN compared to MSY (cf. Eq. 1 and Figure SI-1 in Supporting Information). Moreover, much
266 higher NL and total reductions (TR) were obtained at BCN compared to MSY.

267 Following the MK test, at MSY station the PM_1 fraction from OPC showed non-statistically significant decreasing
268 trend (-1.25 %/yr), whereas for the PM_{10} fraction (OPC) no trend was observed (0.0 %/yr). The magnitude of the
269 trends of PM_{10} and $PM_{2.5}$ concentrations at MSY from gravimetric measurements (-0.47 %/yr and -1.87 %/yr,
270 respectively) confirmed what observed using data from OPC (0.00 %/yr and -1.78 %/yr, respectively).
271 Similarities were also observed between OPC and gravimetric measurements of $PM_{2.5}$ and PM_{10} at BCN (cf.
272 Table 1). Thus, despite the different data coverage the magnitudes of the trends calculated from OPC and
273 gravimetric measurements were very similar. We will show later (*Paragraph 4.1*) that despite the fact that the
274 gravimetric concentrations of PM_{10} at MSY only slightly decreased monotonically with time (-0.47 %/yr with
275 $p>0.1$; cf. Table 1), the contributions from specific PM_{10} pollutant sources from PMF model related with
276 anthropogenic activities showed non-linear (i.e. exponential) statistically significant decreasing trends. For
277 example the *Ammonium sulfate* source contribution to PM_{10} at MSY decreased at the rate of -2.02 %/yr with
278 $p<0.05$ from MK test and double exponential fit of the data was needed; cf. Table 5). At MSY the PM_{1-10} and
279 $PM_{2.5-10}$ size fractions showed non-statistically significant increasing trends of around 0.9 %/yr and 0.62 %/yr,
280 respectively. The decreasing trends of these two PM size fractions at BCN (-2.34 %/yr and -2.18 %/yr for PM_{1-10}
281 and $PM_{2.5-10}$, respectively) were statistically significant however, as already noted, these decreases were largely
282 explained by the change of the BCN measuring station in 2009. Moreover, at MSY non significant decreasing
283 trends were observed for the ratio PM_1/PM_{10} , with magnitude of -1.25 %/yr and for the ratio $PM_{2.5/10}$ decreasing
284 at the rate of -0.62 %/yr. At MSY, on average, the residual component (RC) was quite low and around 8-26% for
285 all PM fractions. Total reductions at MSY (TR) ranged from 8-12% for PM_{10} (not statistically significant) to 24%
286 for $PM_{2.5}$ (statistically significant at $p<0.1$).

287

288 3.2 Trends of PM: Comparison among different periods

289 In this section we compared the magnitude of the trends of gravimetric $PM_{2.5}$ concentrations at MSY over
290 different periods (2002-2010; 2004-2014 and 2002-2014) in order to evaluate the effects of meteorology-driven
291 interannual variability on PM concentrations and trends. Note that the period 2004-2014 was the period chosen
292 for trends analysis in this study given that gravimetric $PM_{2.5}$ measurements at BCN were available since 2004.
293 Conversely, at MSY $PM_{2.5}$ gravimetric measurements started in 2002. Figure 2 shows the trends of $PM_{2.5}$
294 concentrations at MSY calculated using both MK (Fig. 2a) and ME (Fig. 2b) fits for the three different periods.
295 The period 2002-2010 was the period considered in the paper from Cusack et al. (2012) presenting the trends of
296 $PM_{2.5}$ gravimetric mass and chemical species in $PM_{2.5}$ at MSY. The period 2002-2014 is the largest period
297 available so far at MSY with $PM_{2.5}$ filter measurements. The trend observed at MSY for the $PM_{2.5}$ fraction during
298 2004-2014 confirmed what already observed by Cusack et al. (2012) at the same station for the period 2002 –
299 2010. In Cusack et al. (2012) the MK test provided a decreasing trend of around -3.4 %/yr at 0.01 significance



300 level during 2002 – 2010. Considering the period 2004 – 2014, a decreasing trend of -1.87 %/yr at 0.1
301 significance level was observed. Thus, a statistically significant trend for PM_{2.5} at regional level can be confirmed
302 even considering different periods. However, the difference observed in the magnitude of the trends during
303 2004-2014 compared to the results provided by Cusack et al. (2012) suggested that meteorology (in this case a
304 large increase in 2012; cf. Figure 2), changing from year to year, also determined the degree of comparability of
305 trends observed over different periods.

306 As reported in Fig. 2b, the PM_{2.5} trends were linear for the three considered periods (1.2% < NL < 1.5%; cf. Table
307 1) and ME fits did not differ very much from MK fits (Fig. 2a). Following the MK and ME fits, the trends were
308 similar for the periods 2004 – 2014 and 2002 – 2014, whereas results were different for the period 2002 – 2010
309 (Cusack et al., 2012). MK test provided magnitudes of the trends of -1.87 %/yr (p<0.1) and -2.26 %/yr (p<0.05)
310 for 2004 – 2014 and 2002 – 2014, respectively. Conversely, the magnitude of the trend for the period 2002 –
311 2010 was higher in absolute values (-3.42 %/yr with p<0.01). Consequently, following the ME test, the
312 characteristic times (τ) of the periods 2004 – 2014 (31.7 yr) and 2002 – 2014 (34.2 yr) were similar and both
313 were higher compared with τ_1 calculated for the period 2002 – 2010 (19.3 yr). Consequently, the higher TR was
314 observed for the period 2002 – 2010 (34%) for which the highest slope was also observed following both MK
315 and ME tests. The RC was the lowest (9%) for the period 2002 – 2010 compared with 2004 – 2014 and 2002 –
316 2014 (15-16%). The differences observed in the magnitude of the trends and residual components for the three
317 periods are mostly due to the increase in the PM_{2.5} concentrations observed in 2011-2012 when mean PM_{2.5}
318 reached around 15 $\mu\text{g}/\text{m}^3$ similar to the concentrations measured during 2002 – 2004 (around 14-16 $\mu\text{g}/\text{m}^3$).
319 Thus, over relatively short periods (9 -11 yr), the effects of just one meteorologically different year were clearly
320 visible. Despite this, we highlight that a statistically significant trend was observed thus confirming the
321 effectiveness of mitigation measures together with the effect of the economic crisis in Spain from 2008.

322

323 3.3 Trends of chemical species

324 The trends of the concentrations (using annual averages) of chemical species at BCN and MSY are reported in
325 Table 2 (for PM₁₀) and Table 3 (for PM_{2.5}). Figure 3 (for BCN) and Figure 4 (for MSY) show the trends of chemical
326 species in PM₁₀.

327 Here we assume that the change of the station in BCN in 2009 affected the trends of the concentrations of Cr,
328 Cu, Sn and Sb (traffic tracers), Al₂O₃, Ca, Mg, Ti, Rb, Sr (crustal elements related with both natural and
329 anthropogenic sources) and Fe (traffic and crustal tracer). These chemical species were highlighted in yellow in
330 Tables 2 and 3.

331 Figure 3 shows the impact of the change of the station for some of the aforementioned species in the year
332 2009. However, this change did not affect other species reported in Tables 2 and 3 and in Fig. 3, which had less
333 local character. These are SO₄²⁻, NH₄⁺, V, Ni (related with heavy oil combustion in the study area according to



334 source apportionment results, cf. Par. 4), Pb, Cd, As and Zn (related with industrial/metallurgy activities), Na and
335 Cl (sea spray), and NO_3^- . Although nitrate particles in Barcelona were mainly from traffic, the concentrations of
336 these particles were not strongly affected by the change of the station due to their secondary origin. For the
337 aforementioned reasons the comparison between BCN and MSY will be performed only using species (and PMF
338 sources) not affected by the change of the station in BCN. The MSY station will be considered as reference
339 station given that no location changes occurred at this monitoring site during the study period.

340 For the industrial tracers (Pb, Cd, As) the trends were similar in both PM fractions at both BCN and MSY.
341 Following the MK test, the decreasing trends in PM_{10} fraction were statistically significant and ranged between -
342 3.43 %/yr (Cd and As; $p < 0.001$) to -3.74 %/yr (Pb; $p < 0.001$) at BCN and from -3.11 %/yr (Pb; $p < 0.01$) to -3.74
343 %/yr (As; $p < 0.001$) at MSY. In $\text{PM}_{2.5}$ the magnitude of the trends were similar and ranged between -3.58 %/yr
344 (Cd; $p < 0.001$) and -4.05 %/yr (Pb; $p < 0.001$) at BCN and between -3.27 %/yr (As; $p < 0.01$) and -3.74 %/yr (Pb;
345 $p < 0.001$) at MSY. Similar magnitude of the trends for these species in both PM fractions at both sites confirmed
346 the common origin of these elements and the impact at regional scale of industrial sources.

347 However, it can be noted that the trends were not linear and the NL parameters were always higher than 10%
348 for Cd, Pb and As with the exception of As at MSY in PM_{10} (cf. Tables 2 and 3). Thus, for these industrial tracers
349 single or double exponential fits were on average needed indicating that the trends were not gradual and
350 consistent over time and that the effectiveness of the control measures for these pollutants were stronger at
351 the beginning of the period under study (2004-2009 approximately) compared to the end of the period (Figs. 3
352 and 4). This is also evident by comparing the linear MK fit (dashed black line) with the ME fit (red lines) in Figs. 3
353 and 4. Note that at BCN a double exponential (DE) fit was needed to simulate the trends of Pb and Cd
354 concentrations in PM_{10} likely because of the proximity of BCN measuring station to industrial emissions
355 compared to MSY station. For these industrial species in PM_{10} one of the two characteristic times (τ) was slightly
356 negative (cf. Tables 2) indicating both a slight increase of the simulated Pb and Cd concentrations in 2013-2014
357 and the strong decrease at the beginning of the period under study. Interestingly, as shown later, the PM_{10}
358 *Industrial/metallurgy* source contribution at BCN also showed a DE decreasing trend. The decrease observed for
359 Pb, Cd and As may be attributed to a decrease in the emissions from industrial production (smelters, Querol et
360 al., 2007) at a regional scale around Barcelona. The implementation of the IPPC Directive in 2008 in Spain is the
361 most probable cause for this downward trend. In PM_{10} the TR from ME test ranged between 67% for As and
362 73% for Pb, at BCN, and from 48% for As and 72% for Cd, at MSY. In $\text{PM}_{2.5}$ TRs were similar to those observed in
363 PM_{10} as expected given the general fine size mode of these industrial tracers (Table 1 and 2). The RC were quite
364 low and never exceeded 18% thus suggesting the goodness of the exponential fits used to study the trends of
365 the measured specie concentrations.

366 The comparison among the different ME trends in terms of characteristic times (τ) is complicated by the fact
367 that τ is especially sensitive to the noise introduced by the inter-annual variability over the period considered
368 here (11 years). However, some interesting features can be observed. Characteristic times in $\text{PM}_{2.5}$ were very



369 similar for Pb and Cd at both stations (between 6.08 yr and 6.81 yr; cf. Table 3). For As in PM_{2.5} the characteristic
370 times were similar between BCN (9.00 yr) and MSY (8.56 yr) but both were higher compared to Cd and Pb, due
371 to the slightly less intense exponential downward trend observed for As compared to Cd and Pb. Note that the
372 PMF analysis (cf. Paragraph 4) revealed that the concentrations of As were explained by multiple sources
373 (especially at BCN) whereas the *Industrial/metallurgy* source alone explained more than around 70% of Pb and
374 Cd concentrations (not shown). In PM₁₀ in Barcelona the characteristic decreasing times for Pb, Cd and As were
375 similar to those calculated at the same station in PM_{2.5} (despite the different exponential fits used), whereas at
376 MSY the PM₁₀ characteristic times were slightly higher compared with PM_{2.5} especially for As. It should be
377 considered that experimental uncertainties might also contribute to the observed differences in the
378 characteristic decreasing times over the period considered. Moreover, different sampling days for PM₁₀ and
379 PM_{2.5} together with possible sources of coarse As might also contribute to the observed differences.

380 In BCN the magnitude of the trend of PM₁₀ Zn was -3.74 % (p<0.001), from the MK test, and it was comparable
381 with the magnitudes estimated for As, Cd and Pb. However, following the ME test, the trend was linear (NL=6%)
382 and the total reduction was lower (TR=50%) compared to the other industrial tracers. In PM_{2.5} the magnitude of
383 the trend of Zn was lower (-2.65 %/yr; p<0.01) compared with As, Cd and Pb and, again, the trend was linear
384 (NL=5%) and the total reduction (TR=46%) was low compared to the other industrial tracers. At MSY, Zn in PM₁₀
385 showed no statistically decreasing linear trend (-1.40 %/yr; NL = 1%) with low TR of around 23%. Thus PM₁₀ Zn
386 behaved clearly differently compared with As, Pb and Cd. The same was observed in PM_{2.5} at MSY where the
387 magnitude of the trend for Zn (-2.02 %/yr; p<0.1 from MK test) was lower compared with As, Cd and Pb and
388 double exponential fit was needed following the ME test. As reported in Table 2, the two characteristic times
389 of the trend of Zn in PM_{2.5} at MSY were positive and very much different. The exponent with lowest τ (0.21) was
390 needed to explain the strong decrease observed for PM_{2.5} Zn between 2004 and 2005 (Figure SI-2). This
391 different behavior of Zn was likely due to the fact that Zn had multiple origins at both sites being related with
392 both industrial/metallurgy and road traffic emissions.

393 The concentrations of V and Ni in Barcelona in PM₁₀ showed similar trends decreasing at a rate of -3.11 %/yr
394 (p<0.001) and -3.43 %/yr (p<0.001), respectively, following the MK test. Both elements had single-exponential
395 decreasing trends (NL = 12% and 11% for V and Ni, respectively) with very similar decreasing times (10.04 yr and
396 10.61 yr, respectively), TR (63% and 61%, respectively) and RC (17% and 16%, respectively), thus conforming the
397 common origin of these two elements. In PM_{2.5} in Barcelona, the magnitude of the decreasing trends, following
398 the MK test, were slightly lower compared with PM₁₀ (-2.96 %/yr and -3.11 %/yr for V and Ni, respectively;
399 p<0.01) and the trends were linear (NL = 9% for both elements). Characteristic times, TR and RC in PM_{2.5} for V
400 and Ni in BCN were similar to those calculated in PM₁₀. Again we recall that the comparison of the fitting
401 parameters in PM₁₀ and PM_{2.5} might be affected by different number of samples available for these PM size
402 fractions. At MSY, V and Ni showed similar trends as in BCN in both PM fractions. The concentrations of V
403 decreased at the rate of -3.27 %/yr (p<0.01; linear trend with NL = 7%) and -2.65 %/yr (SE trend with NL = 10%)
404 in PM₁₀ and PM_{2.5}, respectively. The concentrations of Ni decreased at the rate of -3.11 %/yr (p<0.01; linear



405 trend with NL = 5%) and -2.80 %/yr (SE trend with NL = 13%) in PM_{10} and $PM_{2.5}$, respectively. Moreover, the
406 characteristic times τ , TR and RC for V and Ni calculated at MSY were similar to those calculated at BCN.

407 As stated before the trends for Cr, Sn, Cu and Sb, typical traffic tracers, were studied only for MSY station as a
408 consequence of the change of the station in BCN in 2009. Sn and Cu in PM_{10} at MSY showed very similar
409 behavior, both decreasing at the rate of -2.34 %/yr ($p < 0.05$) with linear trends ($2\% < NL < 4\%$) and quite similar
410 TR (31-45%) and RC (15-19%). In $PM_{2.5}$, the concentrations of Sn and Cu at MSY showed marked trends
411 compared with PM_{10} , decreasing at -3.74 %/yr ($p < 0.001$) and -3.27 %/yr ($p < 0.01$), respectively. In $PM_{2.5}$ the
412 trends were DE for Sn (see. Figure SI-3) and SE for Cu and TR (67-76%) and RC (9-13%) were similar for both
413 elements. The DE trend for $PM_{2.5}$ Sn at MSY was characterized (as for Zn) by a strong decrease between 2004
414 and 2005 and positive characteristic times (0.23 yr and 11.79 yr; cf. Figure SI-3). For Cr the situation was
415 different compared to Sn and Cu and in PM_{10} at MSY Cr showed no trend (0.00 %/yr). In $PM_{2.5}$ a slight and not
416 statistically significant decreasing trend was detected for Cr concentrations (-1.18 %/yr; $p > 0.1$) which was linear
417 following the ME fit. In $PM_{2.5}$ the TR (31%) calculated for Cr was lower compared to Sn and Cu.

418 Sulfate (SO_4^{2-}) and ammonium (NH_4^+) particles concentrations showed very similar behavior in both $PM_{2.5}$ and
419 PM_{10} size fractions, due to their fine nature, at both sites. In BCN the magnitude of the trends were -3.74 %/yr
420 ($p < 0.001$) and -3.58 %/yr ($p < 0.001$) for SO_4^{2-} and NH_4^+ , respectively. Both trends were SE with very similar
421 characteristic times (9.64-9.81 yr), NL (12%), TR (64-65%) and RC (12-14%). Very similar values were obtained
422 for these two species in $PM_{2.5}$ at BCN (cf. Table 3). At MSY both the magnitude of the trends of SO_4^{2-} and NH_4^+
423 from MK test and their statistical significance were lower compared to BCN in both fractions. The trends were
424 linear for SO_4^{2-} in both fractions and it was SE for NH_4^+ . These differences could be explained by the distance of
425 MSY to direct specific sources of sulfate, such as shipping, compared to BCN, thus slightly reducing the
426 magnitude and the statistical significance of the trend of SO_4^{2-} at regional level. Similar result was observed for
427 the contribution of the *Ammonium sulfate* source at both sites (cf. Table 5) with slightly higher magnitude of the
428 trend observed at BCN compared to MSY. Possible reasons for the observed reduction in the concentrations of
429 ambient sulfate in and around Barcelona will be discussed later.

430 Fine NO_3^- (Table 3) showed very similar trends at both sites (-3.43 and -3.58 %/yr at MSY and BCN, respectively,
431 from MK test) with high statistical significance ($p < 0.001$). At both stations NO_3^- trends were SE and showed
432 similar τ (5.81 yr and 7.61 yr), TR (82% and 73%) and RC (21% and 16%). In PM_{10} the trends of NO_3^- at BCN and
433 MSY were similar to those observed in $PM_{2.5}$ (-3.11 %/yr with $p < 0.01$ from MK test). Following the ME test the
434 TR for PM_{10} NO_3^- were lower (54% at MSY and 64% at BCN) compared to $PM_{2.5}$ and the characteristic times in
435 PM_{10} were also lower compared to $PM_{2.5}$ at both sites. Thus, we deduced from ME analysis that fine NO_3^- had a
436 more pronounced downward trend compared to PM_{10} NO_3^- and mainly at MSY where τ $PM_{2.5}$ and τ PM_{10} were
437 5.81 yr and 12.71 yr, respectively. As reported in *Paragraph 4.1* statistically significant decreasing trends were
438 observed also for the *Ammonium Nitrate* source contributions at both sites. Possible reasons for the observed



439 decreases of NO_3^- concentrations and *Ammonium Nitrate* source contributions will be discussed in *Paragraph*.
440 4.1.

441 As for Cr, Sn, Sb and Cu, the trends of mineral species (Al_2O_3 , Ca, Fe) were studied only at MSY station. For these
442 elements, linear (with the exception of Al_2O_3 in $\text{PM}_{2.5}$ which was SE) and statistically significant decreasing
443 trends (with the exception of Ca in $\text{PM}_{2.5}$ with $p>0.1$) were detected. On average the TR were higher in the fine
444 fraction, ranging from 50% for Ca to 66% for Al_2O_3 , compared to PM_{10} (16-38% cf. Table 2) thus likely suggesting
445 a decrease with time of the concentrations of anthropogenic mineral species from specific sources such as
446 cement and concrete production and production works. In fact, coarse mineral matter at regional background
447 sites is mainly of natural origin. Downward decreasing trend for mineral matter contribution in $\text{PM}_{2.5}$ at MSY
448 was also reported by Cusack et al. (2012) for the period 2002 – 2010 at the same station. It is probable that
449 variations in meteorological conditions from one year to another (i.e. intensity and frequency of Saharan dust
450 outbreaks) might also explain the observed trend of mineral tracers at regional level.

451 The concentrations of Cl^- did not show statistically significant trends in both fractions and at both sites due to its
452 main natural origin. Conversely, following the MK test, slightly statistical significant decreasing trends were
453 observed for Na at both sites and in both fractions with the exception of Na in PM_{10} at MSY for which no trend
454 was detected.

455 Finally, at MSY neither OC nor EC concentrations showed statistically significant trends (not shown). Consider
456 that the concentrations of EC at MSY are very low and around at $0.2\text{-}0.3 \mu\text{g}/\text{m}^3$ as annual mean. Both
457 anthropogenic activity and biomass burning were expected to contribute to this chemical specie. Concerning OC
458 the lack of trend was probably due to the contribution from biogenic sources (and meteorology) to the
459 concentration of this specie at regional level.

460

461 4. PMF source profiles and contributions

462 Eight and seven sources were detected at BCN and MSY, respectively, in PM_{10} from PMF model. The absolute
463 and relative contributions of these sources to the measured PM_{10} mass are reported in Figure 5 and Table 4.
464 The chemical profiles of the detected sources were reported in Supporting Information (Figure SI-4).

465 Some of these sources were common at both BCN and MSY. These are: *Ammonium Sulfate* (secondary inorganic
466 source traced by SO_4^{2-} and NH_4^+ and contributing $3.95 \mu\text{g}/\text{m}^3$ (23.7%) and $4.67 \mu\text{g}/\text{m}^3$ (13.7%) at MSY and BCN,
467 respectively), *Ammonium nitrate* (secondary inorganic source traced by NO_3^- and NH_4^+ and contributing 1.31
468 $\mu\text{g}/\text{m}^3$ (7.9%) and $4.45 \mu\text{g}/\text{m}^3$ (13.1%) at MSY and BCN, respectively), *V-Ni bearing* source (traced mainly by V, Ni
469 and SO_4^{2-} it represents the direct emissions from heavy oil combustion and contributed $0.71 \mu\text{g}/\text{m}^3$ (4.3%) and
470 $3.32 \mu\text{g}/\text{m}^3$ (9.8%) at MSY and BCN, respectively), *Mineral* (traced by typical crustal elements such as Al, Ca, Ti,
471 Rb, Sr and contributing $2.70 \mu\text{g}/\text{m}^3$ (16.2%) and $4.61 \mu\text{g}/\text{m}^3$ (13.6%) at MSY and BCN, respectively), *Aged marine*



472 (traced by Na and Cl mainly with contributions from SO_4^{2-} and NO_3^- and contributing $1.76 \mu\text{g}/\text{m}^3$ (10.6%) and
473 $5.73 \mu\text{g}/\text{m}^3$ (16.9%) at MSY and BCN, respectively). Sources detected at MSY but not at BCN were:
474 *Industrial/Traffic* source (traced by EC, OC, Cr, Cu, Zn, As, Cd, Sn, Sb and Pb it includes mixed contributions from
475 anthropogenic sources such as road traffic and metallurgic industries and contributed $1.43 \mu\text{g}/\text{m}^3$ (8.6%)) and
476 *Aged organics* (traced mainly by OC and EC with maxima in summer indicating mainly a biogenic origin and
477 contributing $3.78 \mu\text{g}/\text{m}^3$ (22.7%)). The ratio OC:EC in the *Industrial/Traffic* and *Aged organic* source profiles at
478 MSY were 4.2 and 11.7, respectively, thus indicating a strong influence of aged particles in the latter source with
479 the former source being more fresh. The statistic of the OC:EC ratio based on chemical data at MSY is reported
480 in Supporting Information (Figure SI-5). Mean and median values of OC:EC ratio at MSY were 9.1 and 7.8,
481 respectively.

482 Finally, some sources were detected at BCN but not at MSY: *traffic* (traced by C_{nm} , Cr, Cu, Sb and Fe mainly and
483 contributing $5.14 \mu\text{g}/\text{m}^3$ (15.1%)), *road/work resuspension* (traced by both crustal elements, mainly Ca, and
484 traffic tracers such as Sb, Cu and Sn and contributing $4.25 \mu\text{g}/\text{m}^3$ (12.5%)) and *Industrial/metallurgy* (traced by
485 Pb, Cd, As and Zn and contributing $0.96 \mu\text{g}/\text{m}^3$ (2.8%).

486 A sensitivity study was performed in order to better interpret the PMF sources at BCN. In fact, for the period
487 2007 – 2014 separate OC and EC concentration measurements were available and a PMF was performed. The
488 comparison between the PMF source contributions obtained using the period 2007-2014 (separate OC and EC
489 measurements) and the whole period (2004-2014; C_{nm} (non-mineral carbon) available) is reported in Supporting
490 Information (Figure SI-6). As reported in Figure SI-6 the differences in source contribution and R^2 ranged
491 between -3% (*Mineral* source) and +20% (*Industrial* source) and 0.894 to 0.997, respectively, thus confirming
492 the correct interpretation of the 2004-2014 PMF sources where C_{nm} was used. The OC:EC ratio in the *Traffic*
493 source from 2007-2014 PMF was 1.70 (cf. Figure SI-7) whereas the mean and median OC:EC ratio from
494 chemistry data were 2.5 and 2.3, respectively, thus being in agreement with the contribution of fresh particles
495 from *Traffic* source at BCN.

496

497 **4.1 Trends of PM_{10} source contributions: annual averages**

498 Figures 6 and 7 and Table 5 show the results from MK and ME test applied to the annual averages of PM_{10}
499 source contributions at BCN and MSY. Following the MK test the source contributions that showed statistically
500 significant downward trends at both stations were *Ammonium sulfate*, *Ammonium nitrate*, and *V-Ni bearing*
501 sources. Moreover, statistically significant decreasing trends were observed for the *Industrial/Traffic* source
502 (including traffic and industrial emissions at MSY) and the *Industrial/metallurgy* source (at BCN). These sources
503 were clearly linked with anthropogenic activities and the observed decreasing trends confirmed the
504 effectiveness of pollution control measures discussed before and the possible effect of the economic crisis. The
505 contributions of these four sources at BCN were not affected by the change of the station in 2009 and,



506 consequently, are discussed here. However, as already noted we cannot study trends for *Traffic, Road/work*
507 *resuspension* and *Mineral* source contributions at BCN.

508 Consistently with the trends of SO_4^{2-} , NO_3^- and NH_4^+ (Table 2), *Ammonium sulfate* and *Ammonium nitrate* source
509 contributions in PM_{10} showed highly statistically significant decreasing trends at both stations (Table 5). The
510 trends from MK test were -2.49% /yr ($p < 0.05$) and -3.74% /yr ($p < 0.001$) for *Ammonium sulfate* and *Ammonium*
511 *nitrates* contributions, respectively, at BCN and -2.02% /yr ($p < 0.05$) and -3.27% /yr ($p < 0.01$), respectively, at
512 MSY. At both stations the trend of the contribution of the *Ammonium sulfate* source to PM_{10} was DE (Double
513 Exponential) with two positive characteristic times (τ ; Table 5) one of which was lower than the other
514 (especially at BCN) indicating a stronger decrease at the beginning of the considered period (cf. Figures 6 and 7).
515 Thus, the decrease over time of the contribution from the *Ammonium sulfate* source was not gradual and
516 monotonic. Note that at MSY there was a small statistically significant difference between SE and DE fits.
517 However, the DE fit was chosen reducing considerably the RC for this source. The TR was quite similar at both
518 sites: 67% at BCN and 51% at MSY and the RC was low at both sites (16-21%) again demonstrating the goodness
519 of the used fits. The observed decrease in the *Ammonium sulfate* source contribution may be attributed to the
520 legislation that came into force in 2007-2008 in Spain, the EC Directive on Large Combustion Plants, which
521 resulted in the application of flue gas desulfurization (FGD) systems in a number of large facilities in 2007-2008
522 in Spain. Moreover, from 2008 on, the use of heavy oils and petroleum coke for power generation was
523 forbidden around Barcelona, thus only natural gas was allowed to this end according to the 2008 Regional AQ
524 Plan.

525 *Ammonium nitrate* contribution trends were SE (Single Exponential) at both stations with very similar τ (8.96 yr
526 – 8.59 yr), TR (67-69 %) and RC (13-17%). Moreover, it should be noted that the lower MK magnitude (and
527 statistical significance) of the *Ammonium sulfate* contribution trends compared to the trends of the *Ammonium*
528 *nitrate* contributions was confirmed by the different fitting lines needed to fit these trends: double exponential
529 for *Ammonium sulfate* contributions and single exponential for *Ammonium nitrate* contributions. Thus, the
530 contributions to PM_{10} from the *Ammonium nitrate* source showed a more gradual and consistent over time
531 decrease compared to the contributions from the *Ammonium sulfate* source.

532 The decreases observed for the concentrations of nitrates (NO_3^- ; cf. Par. 3.2) and for the contribution from the
533 *Ammonium Nitrate* source were mainly related to the reduction in ambient NO_x concentrations. Figure 8 shows
534 the levels of NO_2 from 2005 to 2014 in South Europe from NASA NO_2 OMI level3 plotted using the Giovanni
535 online data system (Acker and Leptoukh, 2007). In Spain it can be observed a general decrease of the
536 concentrations of NO_2 at regional level due to lower energy consumption mainly related with the financial crisis.
537 The decrease of NO_3^- concentrations and *Ammonium nitrate* source contributions around Barcelona was
538 attributed to the decrease of NO_x emissions mainly from the five power generation plants around the city.
539 Moreover, during 2008-2012 the Regional AQ Plan has driven the implementation of SCRT (continuously



540 regenerating PM traps with selective catalytic reduction for NO₂) and the hybridization and shift to natural gas
541 engines of the Barcelona's bus fleet may have had also an influence in NO_x ambient concentrations.

542 The decreasing trends of the *V-Ni bearing* source from MK analysis were similar at both stations and around -
543 3.11 %/yr at BCN (p<0.01) and -2.96 %/yr (p<0.01) at MSY. The trends were linear (L) at MSY (NL=8%) and SE at
544 BCN (NL=11%). Very similar characteristic times (τ) were observed at both stations for the *V-Ni bearing* source
545 contributions: 10.59 yr at BCN and 11.94 yr at MSY. Interestingly, the τ calculated for the *V-Ni bearing* source
546 were very similar to those calculated for V and Ni species in PM₁₀ (cf. Table 2). The *V-Ni bearing* TR was around
547 61% at BCN and 57% at MSY and RCs were similar (19-25 %). Note that following the MK test the magnitude of
548 the trends for these three sources were on average higher at BCN compared to MSY likely due to the proximity
549 of the BCN measuring station to anthropogenic sources of V and Ni (mainly shipping). The observed decrease in
550 the *V-Ni bearing* source contribution was mainly attributed to the ban of the use of heavy oils and petroleum
551 coke for power generation from 2008.

552 The *Industrial/Metallurgy* source contribution at BCN decreased at the rate of -3.43 %/yr from MK test
553 (p<0.001). As already observed this decrease was mainly attributed to the implementation of IPPC Directives.
554 Moreover, the observed decrease may be attributed to a decrease in the emissions from industrial production
555 (smelters, Querol et al., 2007) at a regional scale around Barcelona. The implementation of the IPPC Directive in
556 2008 in Spain was the most probable cause for this downward trend. Also for this source the trend was DE with
557 one negative characteristic time (cf. Table 5) due to a slight increase of the *Industrial/Metallurgy* source
558 contribution at the end of the considered period. This was consistent with the trends observed for the *Industrial*
559 tracers at BCN (cf. Figure 3 and Table 2). TR and RC for the *Industrial* source contributions at BCN were 56% and
560 11%, respectively. Note again that low RC indicates a good fit of the data using the multi-exponential approach.
561 Interestingly, the contribution of the *Industrial/Traffic* source at MSY had a very similar magnitude of the trend
562 (-3.11 %/yr from MK test with p<0.01) compared to the BCN *Industrial* contribution trend, being both sources
563 traced mostly by the same industrial tracers. Also the TR and RC were similar (54% and 11%, respectively at
564 MSY).

565 At MSY the contribution of the *Aged organics* source increased at the rate of +1.25 %/yr however the trend was
566 not statistically significant. The increasing trend for this source was mainly due to the observed increase in the
567 contribution in the year 2011 when mean annual OC concentration at MSY reached a maximum in the
568 considered 11-yr period (not shown). The *Aged organic* source contribution (likely mainly driven by biogenic
569 POA and SOA formed in these forested regional area in the WMB, cf. Pandolfi et al., 2014) did not show
570 statistically significant trends being these contributions mainly driven by meteorology.

571 The *Mineral* source contribution at MSY showed statistically significant decreasing trend (p<0.1) whereas the
572 *Marine* source contributions showed no-statistically significant trends at both stations this being consistent with
573 the natural origin of this latter source. The statistically significant decreasing trend observed at MSY for the
574 *Mineral* source was in agreement with what observed at the same station by Cusack et al. (2012). This



575 decreasing trend could be due to a possible decrease of the emissions of anthropogenic mineral species from
576 specific sources such as cement and concrete production and construction works.

577 Finally, the possible relationship of the ambient air pollution trends with the emission patterns by sectors is
578 evaluated here using the NECo statistical data for Spain (MINETUR, 2013) as well as of the time trends for SO₂
579 and NO_x emissions evidenced for the NEIs (MAGRAMA, 2013). The primary energy consumption increased by
580 +4% from 2004 to 2007, slightly decreased from 2007 to 2008 (-4%), and markedly decreased in 2009 (-12%
581 with respect to 2007) (Fig. 9). Since 2009, the energy consumption indicator seems to remain constantly low
582 until 2012 with an additional decrease in 2013 and 2014 (around -8% compared to 2009). Oil consumption was
583 fairly constant during 2004–2007 showing an important (-29%) decrease during 2007–2014, without major
584 changes from 2007 to 2008 (-3%). This trend is probably governed by the fuel consumption for traffic road.
585 Natural gas consumption increased (+39%) from 2004 to 2008, and then diminished by -45% in 2014 compared
586 to 2008. Coal consumption remained constantly high from 2004 to 2007 whereas, as for the emissions of SO₂
587 (Fig. 10), a sharp decrease occurred from 2007 to 2008 (-31%), continuing until 2010 (-61% compared to 2007).
588 However, in the period 2011–2014 there was an important increase leading to an average consumption similar
589 to the consumption for the year 2008. Nuclear energy consumption remained relatively constant along the
590 study period, whereas the hydroelectric generation had three maxima in 2010, 2013 and 2014, coinciding with
591 the fall of coal consumption. The 2010 increase of hydroelectric consumption was very remarkable and due to
592 the high rainfall rate of this year. Thus, 2010 was a favorable year for atmospheric dispersion and washout of
593 pollution in Spain, but air quality also improved by lower atmospheric emissions due to the decrease of coal
594 consumption in favor of a hydroelectric growth. Renewable energy consumption increased by 440% from 2004
595 to 2014, with a gradual growth in the NECo.

596

597 5.0 Conclusions

598 PM chemical speciated data collected at two twin stations in NE of Spain (one urban background station and
599 one regional background station) during 2004 – 2014 were used to study trends of source contributions from
600 PMF analysis and of chemical species concentrations. Despite the fact the trends of different PM fractions (PM₁,
601 PM_{2.5} and PM₁₀) were linear during the period under study, the trends of specific chemical elements and source
602 contributions were single or double exponential demonstrating the different effectiveness and time of
603 implementation of different reduction strategies on specific pollutant sources. The contributions that showed
604 statistically significant downward trends at both Barcelona (BCN; UB) and Montseny (MSY; RB) were from
605 *Ammonium sulfate*, *Ammonium nitrate*, and *V-Ni bearing* sources. Moreover, statistically significant decreasing
606 trends were observed for the *Industrial/Traffic* source (at MSY; mixed road traffic and metallurgy) and the
607 *Industrial/metallurgy* source (at BCN). These sources were clearly linked with anthropogenic activities and the
608 observed decreasing trends confirmed the effectiveness of pollution control measures implemented at EU or
609 regional/local levels. Moreover, the economic crisis which started in 2008 in Spain also contributed to the



610 observed trends. The general trends observed for the calculated PMF source contributions well reflected the
611 trends observed for the chemical tracers of these pollutant sources. At both sites the decreasing trends of the
612 *Ammonium sulfate* source contributions were double exponential indicating that the trends were not gradual
613 and consistent with time. In fact, the observed decrease in the *Ammonium sulfate* source contribution was
614 mainly attributed to the EC Directive on Large Combustion Plants implemented from 2008 in Spain, resulting in
615 the application of fuels gas desulfurization (FGD) systems in a number of large facilities. Moreover, the use of
616 heavy oils and petroleum coke for power generation was forbidden around Barcelona from 2008, thus only
617 natural gas was allowed to this end according to the 2008 Regional AQ Plan. Conversely, *Ammonium nitrate* and
618 *V-Ni bearing* source contributions were well fitted by a single exponential curve suggesting a more gradual and
619 consistent with time decreasing trends for these contributions compared to *Ammonium sulfate* source
620 contribution. The decrease observed for the contribution of the *Ammonium Nitrate* source was mainly due to
621 the reduction in ambient NO_x concentrations. In Spain a general decrease of the concentrations of NO₂ at
622 regional level was observed and it was mainly related with the lower energy consumption related with the
623 financial crisis. The decrease of nitrates concentrations and *Ammonium nitrate* source contributions around
624 Barcelona was also attributed to the decrease of NO_x emissions from the five power generation plants around
625 the city. Moreover, a Regional AQ Plan implementing the SCRT (continuously regenerating PM traps with
626 selective catalytic reduction for NO₂) and the hybridization and shift to natural gas engines of the Barcelona's
627 bus fleet may have had also an influence in NO_x ambient concentrations. The magnitude of the decreasing
628 trends of the contributions of the aforementioned sources were always higher at BCN compared to MSY likely
629 because of the proximity of the BCN measurement site to anthropogenic pollutant sources compared to the
630 MSY site.

631

632 **Acknowledgments.**

633 This work was supported by the MINECO (Spanish Ministry of Economy and Competitiveness), the MAGRAMA
634 (Spanish Ministry of Agriculture, Food and Environment), the Generalitat de Catalunya (AGAUR 2014 SGR33 and
635 the DGQA) and FEDER funds under the PRISMA project (CGL2012-39623- C02/00). The research leading to these
636 results has received funding from the European Union's Horizon 2020 research and innovation programme
637 under grant agreement No 654109 and previously from the European Union Seventh Framework Programme
638 (FP7/2007-2013) under grant agreement n° 262254. NO₂ map analyses and visualizations used in this paper
639 were produced with the Giovanni online data system, developed and maintained by the NASA GES DISC. The
640 authors would like to express their gratitude to D. C. Carslaw and K. Ropkins for providing the Openair software
641 used in this paper (Carslaw and Ropkins, 2012; Carslaw, 2012).

642

643



644 **Bibliography**

645 Acker J. G. and G. Leptoukh, *Online Analysis Enhances Use of NASA Earth Science Data*, Eos, Trans. AGU, 88, 2,
646 14-17, 2007.

647 Alastuey, A., Minguillón, M.C., Pérez, N., Querol, X., Viana, M. and de Leeuw, F. (2011). *PM10 Measurement*
648 *Methods and Correction Factors: 2009 Status Report*, ETC/ACM Technical Paper 2011/21, 2011.

649 Amato, F., M. Pandolfi, A. Escrig, X. Querol, A. Alastuey, J. Pey, N. Perez, P.K. Hopke, *Quantifying road dust*
650 *resuspension in urban environment by Multilinear Engine: A comparison with PMF2*, Atmospheric Environment.
651 43 - 17, pp. 2770 - 2780. 06/2009, 2009.

652 Barmpadimos, I., J. Keller, D. Oderbolz, C. Hueglin, A.S.H. Prevot, *One decade of parallel fine (PM_{2.5}) and coarse*
653 *(PM₁₀-PM_{2.5}) particulate matter measurements in Europe: trends and variability*, Atmos Chem Phys, 12 (2012),
654 pp. 3189–3203 <http://dx.doi.org/10.5194/acp-12-3189-2012>.

655 Carslaw, D.C., *The OpenAir manual — open-source tools for analysing air pollution data*, Manual for version 0.5-
656 16, King's College, London (2012).

657 Carslaw, D.C., K. Ropkins, *OpenAir — an R package for air quality data analysis*, Environ Model Softw, 27–28
658 (2012), pp. 52–61.

659 Cusack, M., A. Alastuey, N. Perez, J. Pey, X. Querol, *Trends of particulate matter (PM_{2.5}) and chemical*
660 *composition at a regional background site in the Western Mediterranean over the last nine years (2002–2010)*,
661 Atmos Chem Phys, 12 (2012), pp. 8341–8357 <http://dx.doi.org/10.5194/acp-12-8341-2012> [www.atmos-chem-
662 phys.net/12/8341/2012/]

663 EEA: European Environmental Agency Air quality in Europe — 2013 report, EEA report 9/2013, Copenhagen,
664 1725-9177 (2013) [107 pp. <http://www.eea.europa.eu/publications/air-quality-in-europe-2013>].

665 EEA: European Environmental Agency Air quality in Europe — 2015 report, *Many Europeans still exposed to*
666 *harmful air pollution. Air pollution is the single largest environmental health risk in Europe*, EEA report 11/2015,
667 Copenhagen, 1-7 (2015) [[http://www.eea.europa.eu/media/newsreleases/many-europeans-still-exposed-to-](http://www.eea.europa.eu/media/newsreleases/many-europeans-still-exposed-to-air-pollution-2015)
668 [air-pollution-2015](http://www.eea.europa.eu/media/newsreleases/many-europeans-still-exposed-to-air-pollution-2015)].

669 Escrig, A., Monfort, E., Celades, I., Querol, X., Amato, F., Minguillón, M. C., and Hopke, P. K.: Application of
670 optimally scaled target factor analysis for assessing source contribution of ambient PM₁₀, J. Air Waste
671 Manage., 59(11), 1296–1307, 2009.

672 Gilbert, R.O. 1987 . Statistical Methods for Environmental Pollution Monitoring, Wiley, NY.



- 673 Guerreiro, C., Leeuw, F. de, Foltescu, V., Horálek, J., & European Environment Agency. (2014). *Air quality in*
674 *Europe 2014 report*, Luxembourg: Publications Office. Retrieved from
675 <http://bookshop.europa.eu/uri?target=EUB:NOTICE:THAL14005:EN:HTML>.
- 676 Harrison, R.M., J. Stedman, D. Derwent, *New directions: why are PM10 concentrations in Europe not falling?*,
677 *Atmos Environ*, 42 (3) (2008), pp. 603–606.
- 678 Henschel, S., X. Querol, R. Atkinson, M. Pandolfi, A. Zeca, A. Le Tertre, A. Analitis, K. Katsouyanni, O. Chanel, M.
679 Pascal, C. Bouland, D. Haluza, S. Medina, P.G. Goodman, *Ambient air SO2 patterns in 6 European cities*,
680 *Atmospheric Environment*. 79, pp. 236 - 247. 11/2013, 2013.
- 681 Henschel, S., A. Le Tertre, R.W. Atkinson, X. Querol, M. Pandolfi, A. Zeka, D. Haluza, A. Antonis, K. Katsouyanni,
682 C. Bouland, M. Pascal, S. Medina, P.G. Goodman, *Trends of nitrogen oxides in ambient air in nine European cities*
683 *between 1999 and 2010*, *Atmospheric Environment*. 117, pp. 234 - 241. 09/2015, 2015.
- 684 Kendall, M.G. 1975. *Rank Correlation Methods*, 4th edition, Charles Griffin, London.
- 685 Mann, H.B. 1945. *Non-parametric tests against trend*, *Econometrica* 13:163-171.
- 686 Paatero, P. and Tapper, U.: *Positive Matrix Factorization: a non negative factor model with optimal utilization of*
687 *error estimates of data values*, *Environmetrics*, 5, 111–126, 1994.
- 688 Paatero, P.: *Least squares formulation of robust non-negative factor analysis*, *Chemometr. Intell. Lab.*, 37, 23–
689 35, 1997.
- 690 Paatero, P., Hopke, P. K., Song, X., and Ramadan, Z.: *Understanding and controlling rotations in factor analytic*
691 *models*, *Chemo metrics and Intelligent Laboratory Systems*, 60(1–2), 253–264, 2002.
- 692 Paatero, P. and Hopke, P. K.: *Discarding or downweighting high noise variables in factor analytic models*, *Anal.*
693 *Chim. Acta*, 490, 277–289, doi:10.1016/s0003-2670(02)01643-4, 2003.
- 694 Paatero, P., Hopke, P. K., Begum, B. A., and Biswas, S. K.: *A graphical diagnostic method for assessing the*
695 *rotation in factor analytical models of atmospheric pollution*, *Atmos. Environ.*, 39, 193–201,
696 doi:10.1016/j.atmosenv.2004.08.018, 2005.
- 697 Pandolfi, M., Cusack, M., Alastuey, a. and Querol, X.: *Variability of aerosol optical properties in the Western*
698 *Mediterranean Basin*, *Atmos. Chem. Phys.*, 11(15), 8189–8203, doi:10.5194/acp-11-8189-2011, 2011.
- 699 Pandolfi, M., F. Amato, C. Reche, A. Alastuey, R. P. Otjes, M. J. Blom, X. Querol, *Summer ammonia*
700 *measurements in a densely populated Mediterranean city*, *Atmospheric Chemistry and Physics*. 12, pp. 7557 -
701 7575. 08/2012, 2012.



- 702 Pandolfi, M., G. Martucci, X. Querol, A. Alastuey, F. Wilsenack, S. Frey, C.D. O'Dowd, M. Dall'Osto, *Continuous*
703 *atmospheric boundary layer observations in the coastal urban area of Barcelona during SAPUSS*, Atmospheric
704 Chemistry and Physics. 13 - 9, pp. 4983 - 4996. 05/2013, 2013.
- 705 Pandolfi, M., Querol, X., Alastuey, A., Jimenez, J. L., Jorba, O., Day, D., Ortega, A., Cubison, M. J., Comerón, A.,
706 Sicard, M., Mohr, C., Prévôt, A. S. H., Minguillón, M. C., Pey, J., Baldasano, J. M., Burkhardt, J. F., Seco, R.,
707 Peñuelas, J., van Drooge, B. L., Artiñano, B., Di Marco, C., Nemitz, E., Schallhart, S., Metzger, A., Hansel, A.,
708 Lorente, J., Ng, S., Jayne, J. and Szidat, S.: Effects of sources and meteorology on particulate matter in the
709 Western Mediterranean Basin: An overview of the DAURE campaign, *J. Geophys. Res. Atmos.*, 119(8), 4978–
710 5010, doi:10.1002/2013JD021079, 2014.
- 711 Pérez, N., Pey, J., Castillo, S., Viana, M., Alastuey, A. and Querol, X.: Interpretation of the variability of levels of
712 regional background aerosols in the Western Mediterranean, *Sci. Total Environ.*, 407(1), 527–540,
713 doi:10.1016/j.scitotenv.2008.09.006, 2008.
- 714 Pey, J., Pérez, N., Querol, X., Alastuey, A., Cusack, M. and Reche, C.: Intense winter atmospheric pollution
715 episodes affecting the Western Mediterranean., *Sci. Total Environ.*, 408(8), 1951–9,
716 doi:10.1016/j.scitotenv.2010.01.052, 2010.
- 717 Querol, X., A. Alastuey, T. Moreno, M.M. Viana, S. Castillo, J. Pey, et al., *Spatial and temporal variations*
718 *in airborne particulate matter (PM10 and PM2.5) across Spain 1999–2005*, *Atmos Environ*, 42 (2008), 3694–
719 3979.
- 720 Querol, X., M. Viana, T. Moreno, A. Alastuey, J. Pey, F. Amato, M. Pandolfi, et al., *Scientific bases for a National*
721 *Air Quality Plan* (in Spanish), Colección Informes CSIC, 978-84-00-09475-1, 3 (2012) [349 pp.].
- 722 Querol, X., , A. Alastuey, M. Pandolfi, C. Reche, N. Pérez, M.C. Minguillón, T. Moreno, M. Viana, M. Escudero, A.
723 Orio, M. Pallarés, F. Reina, *2001–2012 trends on air quality in Spain*, *Science of The Total Environment*, 490,
724 (2014), 957–969, doi:10.1016/j.scitotenv.2014.05.074.
- 725 Salvador P., Artiñano B., Viana M., Alastuey A., Querol X.: *Evaluation of the changes in the Madrid metropolitan*
726 *area influencing air quality: analysis of 1999-2008 temporal trend of Particulate Matter*, *Atmos. Environ.*, 57,
727 175-185, 2012.
728
- 729 Sen, P.K., *Estimates of regression coefficient based on Kendall's tau*, *J Am Stat Assoc*, 63 (1968), pp. 1379–1389.
- 730 Shatalov V., Ilyin I., Gusev A., Rozovskaya O., Travnikov O.: *Heavy Metals and Persistent Organic Pollutants:*
731 *development of multi-scale modeling and trend analysis methodology*. EMEP/MSC-E Technical report 1/2015,
732 2015.



733 Smith, D.M.: *Computing single parameter transformations*, Communications in Statistics - Simulation and
734 Computation, 32, 605-618, 2002.

735 Theil, H., *A rank invariant method of linear and polynomial regression analysis, I, II, III*, Proceedings of the
736 Koninklijke Nederlandse Akademie Wetenschappen, SeriesA — Mathematical Sciences, 386-392, 521-525,
737 1397-1412 (1950).

738 Williams, M.L., D. Carslaw, *New directions: science and policy — out of step on NO_x and NO₂?* Atmos Environ, 45
739 (23) (2011), pp. 3911-3912.

740

741

742

743

744

745

746

747

748

749

750

751

752

753

754

755

756

757

758



759 **Table 1:** Mann-Kendall and Multi-exponential trends of different PM fractions from both gravimetry (grav) and optical (OPC)
 760 measurements at BCN (bold italic) and MSY (2004-2014). Type: linear (L), single-exponential (SE), double exponential (DE); a ($\mu\text{g m}^{-3}$) and
 761 τ (yr) are the constant and the characteristic time, respectively, of the exponential fit of the data; NL (%) = Non-Linearity; TR (%) = Total
 762 Reduction; RC (%) = Residual Component. Significance of the trends following the Mann-Kendall test: *** (p-value < 0.001), ** (p-value <
 763 0.01), * (p-value < 0.05), + (p-value < 0.1).

PM _x	PM _x		Mann-Kendall fit		Multi-exponential fit					
	Conc. 2004 ($\mu\text{g m}^{-3}$)	Conc. 2014 ($\mu\text{g m}^{-3}$)	Trend (%/yr)	p-value	type	a ($\mu\text{g m}^{-3}$)	τ (yr)	NL (%)	TR (%)	RC (%)
PM ₁₀ (grav)	41.12	19.16	-3.58	***	L	50.30	11.60	9	58	10
	19.24	13.88	-0.47		L	17.92	79.46	0	12	17
PM _{2.5} (grav)	31.61	13.18	-3.89	***	L	32.41	10.87	9	60	8
	16.18	9.80	-1.87	+	L	14.36	31.70	1	27	16
PM ₁₀ (OPC)	39.06	19.84	-3.43	***	L	45.85	15.62	5	47	11
	18.63	12.34	0.00		L	16.25	115.92	0	8	15
PM _{2.5} (OPC)	27.12	12.86	-3.11	**	L	29.33	15.51	5	53	11
	15.71	9.28	-1.78	+	L	12.46	40.59	0	24	14
PM ₁ (OPC)	20.78	9.05	-3.11	**	L	23.03	13.83	6	51	13
	12.86	6.68	-1.25		L	10.90	37.33	1	23	17
PM ₁₋₁₀ (OPC)	18.29	11.48	-2.34	*	L	22.86	17.92	4	43	16
	5.94	5.51	0.93		L	5.61	-68.77	0	-16	23
PM _{1/10} (OPC)	0.55	0.46	-0.31		L	0.50	135.80	0	7	9
	0.71	0.59	-1.25		L	0.67	70.88	0	13	10
PM _{2.5-10} (OPC)	13.07	7.89	-2.18	*	L	14.72	16.25	5	46	18
	4.09	3.79	0.62		L	3.88	-76.32	0	-14	26
PM _{2.5/10} (OPC)	0.66	0.63	-0.62		L	0.68	396.60	0	2	4
	0.80	0.77	-0.62		L	0.76	288.49	0	3	9

764

765

766

767

768

769

770

771

772

773

774



775 **Table 2:** Mann-Kendall and Multi-exponential trends of different chemical species in PM₁₀ at BCN (bold italic) and MSY. Colour highlights
 776 species in BCN for which trends cannot be studied due to the change of the BCN station in 2009. Type: linear (L), single-exponential (SE),
 777 double exponential (DE); a ($\mu\text{g m}^{-3}$) and τ (yr) are the constants and the characteristic times, respectively, of the exponential data fittings;
 778 NL (%) = Non-Linearity; TR (%) = Total Reduction; RC (%) = Residual Component. Significance of the trends following the Mann-Kendall
 779 test: *** (p-value < 0.001), ** (p-value < 0.01), * (p-value < 0.05), + (p-value < 0.1).

Specie	PM ₁₀ (BCN;MSY)		Mann-Kendall fit		Multi-exponential fit					
	Concentration 2004 ($\mu\text{g m}^{-3}$)	Concentration 2014 ($\mu\text{g m}^{-3}$)	Trend (%/yr)	p-value	type	a ($\mu\text{g m}^{-3}$)	τ (yr)	NL (%)	TR (%)	RC (%)
Pb	0.02685	0.00694	-3.74	***	DE	0.03409 1.64E-5	5.38 -2.09	39	73	10
	0.00481	0.00190	-3.11	**	SE	0.00553	10.22	11	62	13
Cd	0.00043	0.00015	-3.43	***	DE	0.00051 3.36E-8	6.64 -1.48	33	65	11
	0.00017	0.00006	-3.27	**	SE	0.00018	7.92	18	72	16
As	0.00094	0.00036	-3.43	***	SE	0.00118	9.11	14	67	11
	0.00029	0.00017	-3.74	***	L	0.00031	15.39	5	48	10
Zn	0.10584	0.05483	-3.74	***	L	0.11310	14.49	6	50	7
	0.01401	0.00912	-1.40		L	0.01434	38.46	1	23	19
V	0.01116	0.00454	-3.11	**	SE	0.01502	10.04	12	63	17
	0.00328	0.00175	-3.27	**	L	0.00412	13.00	7	54	16
Ni	0.00531	0.00284	-3.43	***	SE	0.00678	10.61	11	61	16
	0.00155	0.00100	-3.11	**	L	0.00180	15.73	5	47	21
Cr	0.00499	0.00316	-2.49	*	L	0.00641	15.38	5	48	18
	0.00102	0.00110	0.00		L	0.00100	127.74	0	8	23
Sn	0.00532	0.00402	-2.02	*	L	0.00745	24.55	2	33	15
	0.00127	0.00057	-2.34	*	L	0.00107	16.97	4	45	15
Cu	0.07064	0.01394	-2.96	**	SE	0.10238	6.18	27	80	30
	0.00420	0.00216	-2.34	*	L	0.00416	26.63	2	31	19
Sb	0.00894	0.00207	-2.96	**	SE	0.01140	6.19	27	80	25
	0.00058	0.00025	-2.80	**	SE	0.00064	10.46	11	62	13
SO ₄ ²⁻	5.74436	2.28596	-3.74	***	SE	6.56033	9.81	12	64	12
	2.84849	1.67712	-2.80	**	L	3.00501	18.54	4	42	19
NO ₃ ⁻	5.07816	1.72401	-3.11	**	SE	6.49890	9.83	12	64	15
	1.80724	0.67419	-3.11	**	L	2.10077	12.71	7	54	14
NH ₄ ⁺	1.92062	0.57008	-3.58	***	SE	1.90645	9.64	12	65	14
	1.14268	0.40135	-2.49	*	SE	1.28868	9.26	13	66	22
Al ₂ O ₃	1.25631	0.42353	-2.34	*	SE	1.83628	8.80	15	68	33
	0.72357	0.46382	-2.18	*	L	0.71956	23.71	2	35	19
Ca	2.34383	0.49357	-2.96	**	SE	3.35120	7.27	21	75	34
	0.42703	0.28279	-2.49	*	L	0.47048	21.07	3	38	17
Fe	0.94101	0.46700	-2.18	*	L	1.21322	11.22	9	59	17
	0.22371	0.14895	-1.71	+	L	0.22198	56.84	0	16	40
Na	1.02188	0.77408	-2.34	*	L	1.13649	28.31	2	30	13
	0.31184	0.33089	0.00		L	0.33531	493.40	0	2	21
Cl	0.85827	0.78893	-1.09		L	0.92544	40.26	1	22	20
	0.17991	0.34437	0.62		L	0.22167	-36.01	1	-32	61

780

781

782

783

784

785

786



787 **Table 3:** Mann-Kendall and Multi-exponential trends of different chemical species in PM_{2.5} at BCN (bold italic) and MSY. Colour highlights
 788 species in BCN for which trends cannot be studied due to the change in the BCN station in 2009. Type: linear (L), single-exponential (SE),
 789 double exponential (DE); a ($\mu\text{g m}^{-3}$) and τ (yr) are the constants and the characteristic times, respectively, of the exponential data fittings;
 790 NL (%) = Non-Linearity; TR (%) = Total Reduction; RC (%) = Residual Component. Significance of the trends following the Mann-Kendall
 791 test: *** (p-value < 0.001), ** (p-value < 0.01), * (p-value < 0.05), + (p-value < 0.1).

Specie	PM _{2.5} (BCN,MSY)		Mann-Kendall fit		Multi-exponential fit					
	Concentration 2004 ($\mu\text{g m}^{-3}$)	Concentration 2014 ($\mu\text{g m}^{-3}$)	Trend (%/yr)	p-value	type	a ($\mu\text{g m}^{-3}$)	τ (yr)	NL (%)	TR (%)	RC (%)
Pb	0.02117	0.00500	-4.05	***	SE	0.02390	6.24	27	80	13
	0.00642	0.00149	-3.74	***	SE	0.00716	6.08	28	81	18
Cd	0.00041	0.00011	-3.58	***	SE	0.00047	6.81	23	77	13
	0.00020	0.00005	-3.58	***	SE	0.00020	6.77	23	77	18
As	0.00069	0.00027	-3.74	***	SE	0.00091	9.00	14	67	11
	0.00029	0.00013	-3.27	**	SE	0.00033	8.56	15	69	19
Zn	0.07500	0.03985	-2.65	**	L	0.07330	16.41	5	46	13
	0.02649	0.01017	-2.02	*	DE	1.53281 0.01377	0.21 22.56	49	68	18
V	0.00823	0.00368	-2.96	**	L	0.01121	11.13	9	59	16
	0.00271	0.00130	-2.65	**	SE	0.00338	10.77	10	60	21
Ni	0.00402	0.00185	-3.11	**	L	0.00498	11.23	9	59	15
	0.00189	0.00080	-2.80	**	SE	0.00205	9.36	13	42	24
Cr	0.00226	0.00155	-1.40		L	0.00297	16.05	5	46	27
	0.00077	0.00062	-1.18		L	0.00104	16.75	4	31	24
Sn	0.00268	0.00188	-2.34	*	L	0.00398	19.87	3	40	16
	0.00157	0.00043	-3.74	***	DE	0.04830 0.00100	0.23 11.79	44	76	9
Cu	0.02747	0.00503	-3.11	**	SE	0.05273	5.32	34	85	43
	0.00394	0.00113	-3.27	**	SE	0.00426	8.99	14	67	13
Sb	0.00300	0.00078	-2.96	**	DE	0.00395 1.6E-6	5.10 -1.98	42	73	18
	0.00053	0.00015	-2.80	**	DE	0.00069 1.3E-6	4.52 -2.50	48	70	16
SO ₄ ²⁻	4.86564	1.92388	-3.74	***	SE	5.64582	9.69	12	64	9
	2.98922	1.43381	-2.96	**	L	3.29195	11.70	9	57	16
NO ₃ ⁻	3.45513	0.86002	-3.58	***	SE	4.14459	7.61	19	73	16
	1.66095	0.29452	-3.43	***	SE	1.96014	5.81	30	82	21
NH ₄ ⁺	2.19735	0.68393	-3.58	***	SE	2.27813	10.53	11	61	15
	1.39366	0.48049	-3.11	**	SE	1.62588	7.94	18	72	14
Al ₂ O ₃	0.46954	0.14567	-2.65	**	SE	0.73949	7.46	20	74	39
	0.30245	0.10153	-2.34	*	SE	0.26678	9.36	13	66	35
Ca	0.65421	0.13737	-2.80	**	SE	1.09283	5.91	29	82	46
	0.11478	0.06540	-1.56		L	0.10688	14.36	6	50	33
Fe	0.32489	0.15007	-1.87	+	SE	0.45302	8.26	16	70	25
	0.09679	0.03716	-2.02	*	L	0.08842	12.20	8	56	31
Na	0.27476	0.17863	-1.87	+	L	0.32279	19.56	3	40	15
	0.13091	0.07252	-2.49	*	L	0.13516	18.56	4	42	19
Cl	0.37296	0.32756	-0.47		L	0.37806	23.25	2	35	49
	0.10917	0.18225	0.00		L	0.16170	-1029.00	0	-1	79

792

793

794

795

796



797 **Table 4:** Source contributions at Barcelona (BCN) and Montseny (MSY)

	BCN [$\mu\text{g}/\text{m}^3$, %]	MSY [$\mu\text{g}/\text{m}^3$, %]
<i>Source</i>		
AgedMarine	5.73; 16.9	1.76; 10.6
Mineral	4.61; 13.6	2.70; 16.2
AmmSulfate	4.67; 13.7	3.95; 23.7
AmmNitrate	4.45; 13.1	1.31; 7.9
V-Ni	3.32; 9.8	0.71; 4.3
Industrial/Metallurgy	0.96; 2.8	
Traffic	5.14; 15.1	
Road/work resuspension	4.25; 12.5	
Aged Organics		3.78; 22.7
Industrial/Traffic		1.43; 8.6

798

799

800

801

802

803

804

805

806

807

808

809

810

811

812

813

814

815

816



817 **Table 5:** Mann-Kendall and Multi-exponential trends of source contributions in PM₁₀ from PMF at BCN (bold italic) and MSY. Highlighted
 818 source contributions at BCN from Mineral, Traffic and Road/work resuspension were excluded from the trend discussion. Type: linear (L),
 819 single-exponential (SE), double exponential (DE); *a* (μg m⁻³) and *τ* (yr) are the constants and the characteristic times, respectively, of the
 820 exponential data fittings; NL (%) = Non-Linearity; TR (%) = Total Reduction; RC (%) = Residual Component. Significance of the trends
 821 following the Mann-Kendall test: *** (p-value < 0.001), ** (p-value < 0.01), * (p-value < 0.05), + (p-value < 0.1).

Source	PM ₁₀ (BCN;MSY)		Mann-Kendall fit		Multi-exponential fit					
	Contribution 2004 (μg m ⁻³)	Contribution 2014 (μg m ⁻³)	Trend (%/yr)	p-value	type	<i>a</i> (μg m ⁻³)	<i>τ</i> (yr)	NL (%)	TR (%)	RC (%)
<i>Ammonium sulfate</i>	10.27	3.38	-2.49	*	DE	12.33 3.82	1.65 105.80	45	67	16
	6.57	3.07	-2.02	*	DE	4.92 3.05	2.44 85.63	27	51	21
<i>Ammonium nitrate</i>	6.99	1.96	-3.74	***	SE	8.54	8.96	14	67	13
	2.03	0.47	-3.27	**	SE	2.44	8.59	15	69	17
<i>V-Ni bearing</i>	4.23	1.84	-3.11	**	SE	5.66	10.59	11	61	19
	0.79	0.44	-2.96	**	L	1.13	11.94	8	57	25
<i>Industrial/Metallurgy (BCN)</i>	1.64	0.71	-3.43	***	DE	1.89 0.0015	7.41 -2.06	29	56	11
<i>Mineral</i>	4.61	3.01	-1.87	+	L	6.53	16.19	12	64	46
	3.46	2.32	-1.71	+	L	3.34	27.46	5	46	34
<i>Marine</i>	5.67	4.91	-1.40		L	6.45	47.09	1	19	14
	1.53	1.89	0.62		L	1.71	107.83	0	-10	24
<i>Industrial/Traffic (MSY)</i>	2.08	1.01	-3.11	**	L	2.18	12.94	7	54	11
<i>Aged Organics (MSY)</i>	3.14	3.26	1.25		L	3.34	-51.05	1	-22	17
<i>Traffic (BCN)</i>	8.21	3.33	-2.65	**	SE	9.87	8.82	15	68	21
<i>Road/work resuspension (BCN)</i>	7.33	0.89	-2.80	**	SE	10.52	6.15	27	80	41

822

823

824

825

826

827

828

829

830

831

832 **Figure Captions:**

833 **Figure 1:** Location of the Barcelona (BCN) and Montseny (MSY) measuring stations. Red full circle highlights the location of the BCN
834 measuring station before 2009. Green full circle highlights the new location of the BCN (from 2009) and MSY measuring stations.

835 **Figure 2:** Mann-Kendall (a) and Multi-exponential (b) fits of $PM_{2.5}$ trends at MSY station for the periods 2002-2010 (as in Cusack et al.,
836 2012), 2004 – 2014 (this work), and 2002 – 2014 (largest period so far available). TZ_MK: Mann-Kendall trend (%/yr); S_MK: significance
837 of Mann-Kendall trend; a_n : multiplicative constant of exponential function ($\mu g/m^3$); τ_n : characteristic time of exponential function (yr);
838 NL: non-linearity (%); TR: total reduction (%); RC: residual component (%). Significance of the trends following the Mann-Kendall test: ***
839 (p-value < 0.001), ** (p-value < 0.01), * (p-value < 0.05), + (p-value < 0.1).

840 **Figure 3:** Mann-Kendall (MK) and Multi-exponential (ME) trends for chemical species at BCN in PM_{10} . Measured concentration (green
841 line); Multi-exponential trend (red line); Multi-exponential residuals (blue line); Mann-Kendall trend (black line); Mann-Kendall residuals
842 (grey line). Trend type: linear (L), single-exponential (SE), double exponential (DE).

843 **Figure 4:** Mann-Kendall (MK) and Multi-exponential (ME) trends for chemical species at MSY in PM_{10} . Measured concentration (green
844 line); Multi-exponential trend (red line); Multi-exponential residuals (blue line); Mann-Kendall trend (black line); Mann-Kendall residuals
845 (grey line). Trend type: linear (L), single-exponential (SE), double exponential (DE).

846 **Figure 5:** Source contributions from PMF model in PM_{10} at Montseny (MSY) and Barcelona (BCN). Mean values during 2004-2014. Values
847 reported are: **Source; $\mu g/m^3$; %.**

848 **Figure 6:** Mann-Kendall and Multi-exponential trends for source contributions in PM_{10} at BCN. Measured concentration (green line);
849 Multi-exponential trend (red line); Multi-exponential residuals (blue line); Mann-Kendall trend (black line); Mann-Kendall residuals (grey
850 line). Trend type: linear (L), single-exponential (SE), double exponential (DE). Highlighted with yellow colour the source contributions at
851 BCN from *Mineral, Traffic and Road/work resuspension* were excluded from the trend discussion.

852 **Figure 7:** Mann-Kendall and Multi-exponential trends for source contributions in PM_{10} at MSY. Measured concentration (green line);
853 Multi-exponential trend (red line); Multi-exponential residuals (blue line); Mann-Kendall trend (black line); Mann-Kendall residuals (grey
854 line). Trend type: linear (L), single-exponential (SE), double exponential (DE).

855 **Figure 8:** NASA NO_2 OMI level 3 plotted using the Giovanni online data system, developed and maintained by the NASA GES DISC.

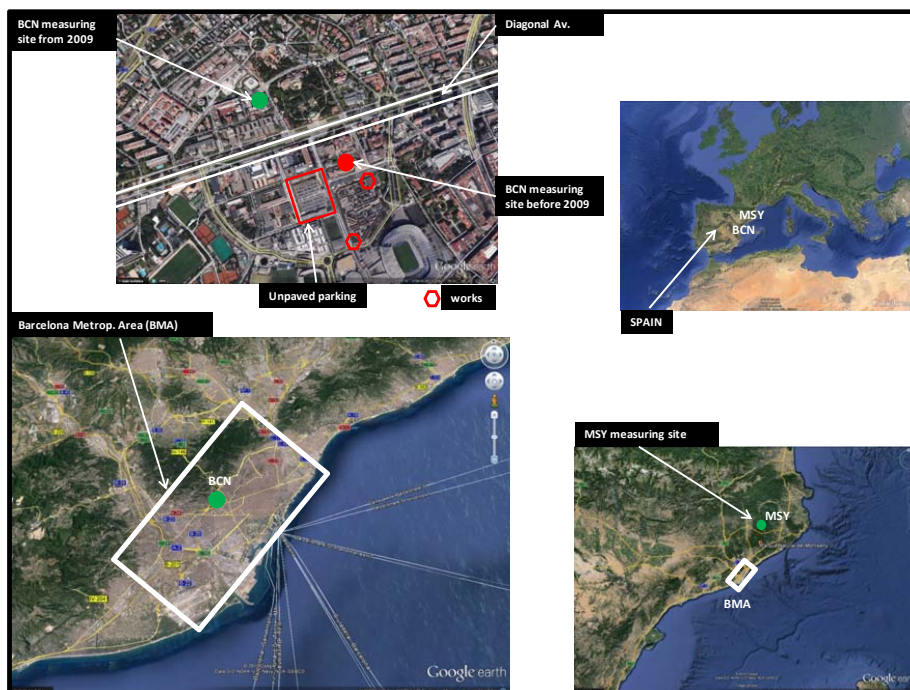
856 **Figure 9:** Annual (2004–2014) energy consumption for Spain (normalized to year 2004). Data from the Spanish Ministry of Industry
857 (MINETUR, 2013).

858 **Figure 10:** Spanish national emission of SO_2 and NO_x (normalized to year 2004).

859

860

861



862

863 **Figure 1**

864

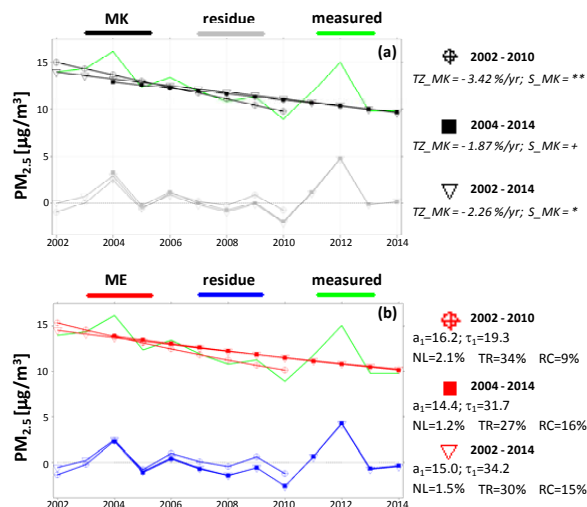
865

866

867

868

869



870

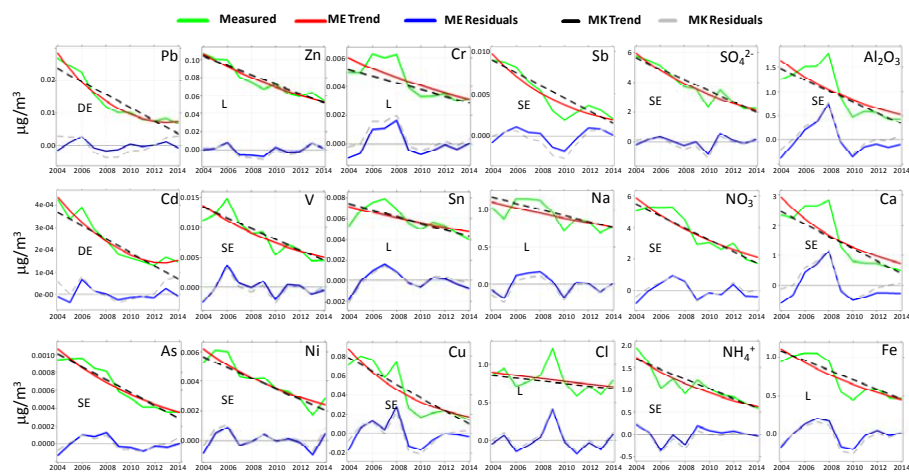
871 **Figure 2**

872

873

874

875



876

877 **Figure 3**

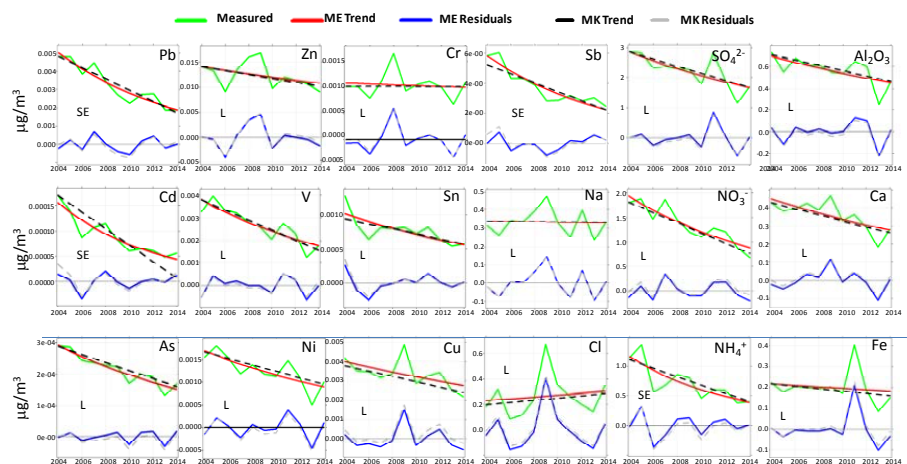
878

879

880



881



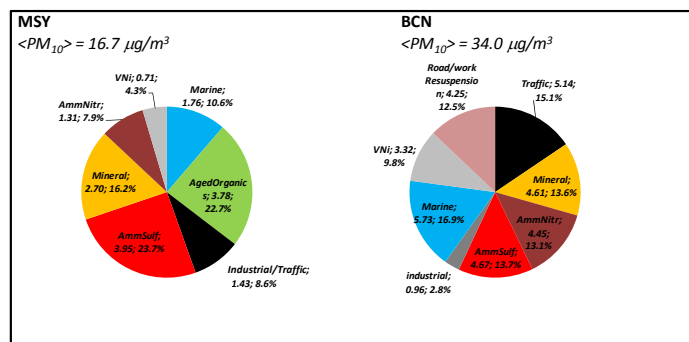
882

883 **Figure 4**

884

885

886



887

888 **Figure 5**

889

890

891

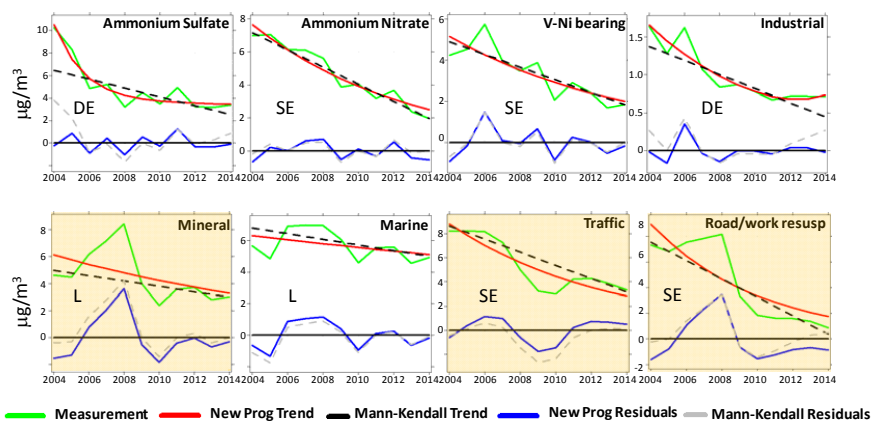
892

893



894

895



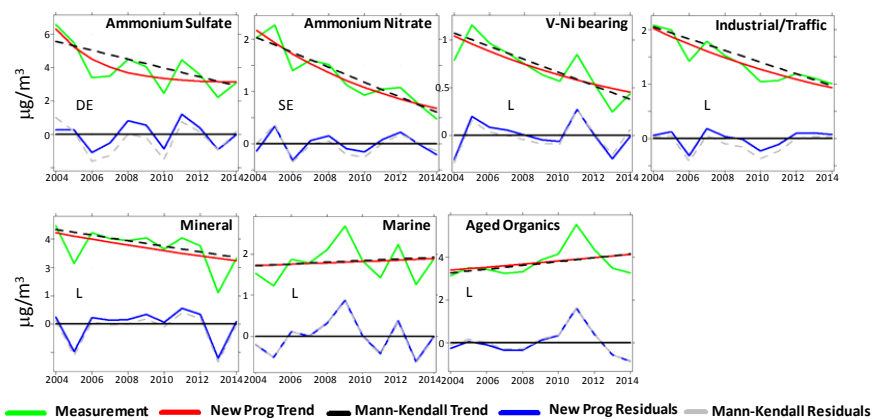
897 **Figure 6**

898

899

900

901



903 **Figure 7**

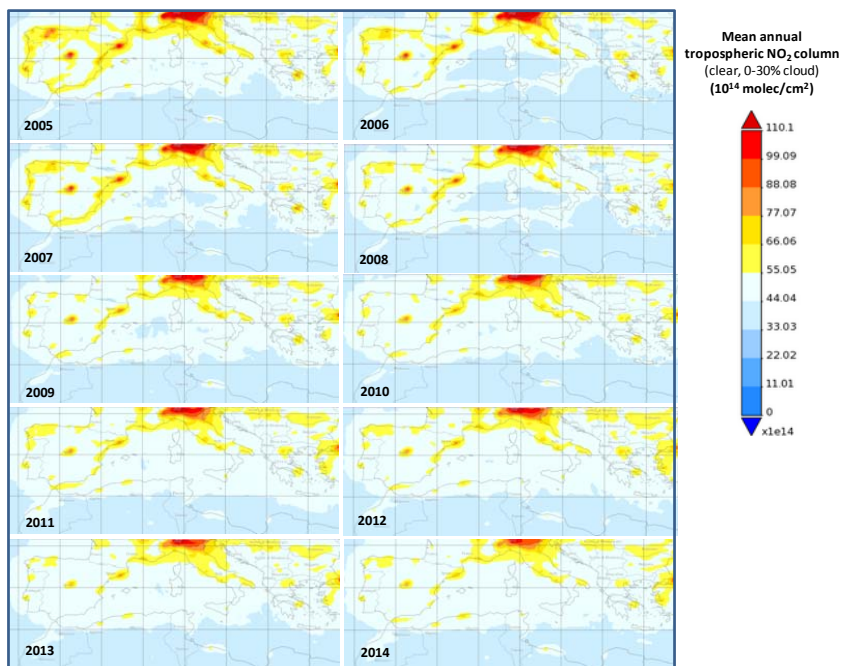
904

905

906



907



908

909 **Figure 8**

910

911

912

913

914

915

916

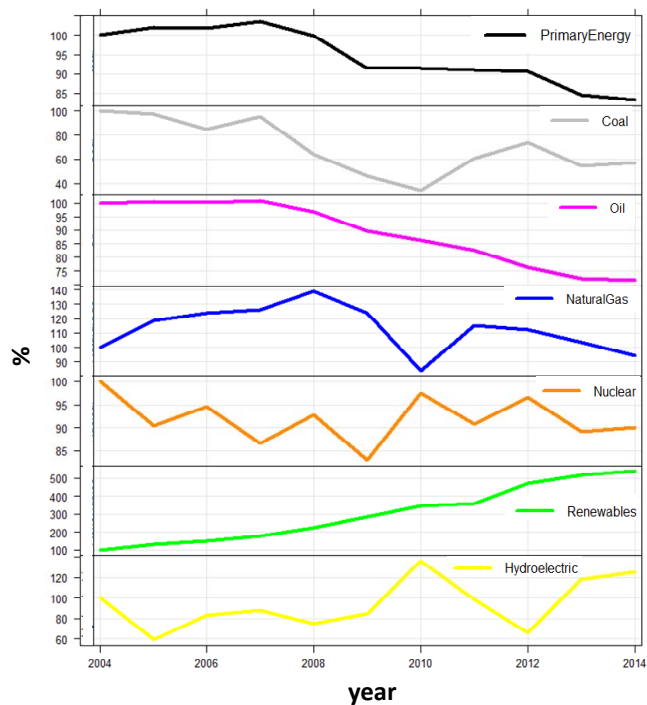
917

918

919

920

921

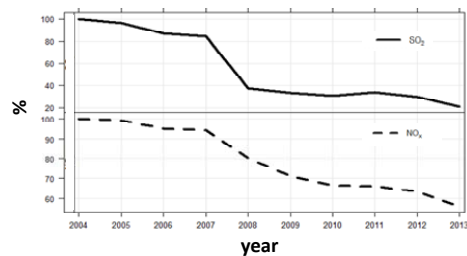


922

923 **Figure 9**

924

925



926

927 **Figure 10**

928

929